Contemporary Physics, 2001, volume 42, number 5, pages 285–314

Science with radioactive beams: the alchemist's dream

W. GELLETLY

Nuclear science is being transformed by a new capacity to create beams of radioactive nuclei. Until now all of our knowledge of nuclear physics and the applications which flow from it has been derived from studies of radioactive decay and nuclear reactions induced by beams of the 283 stable or long-lived nuclear species we can find on Earth. Here we describe first how beams of radioactive nuclei can be created. The present status of nuclear physics is then reviewed before potential applications to nuclear physics, nuclear astrophysics, materials science, bio-medical, and environmental studies are described.

1. Introduction

The study of nuclear physics demands beams of energetic particles to induce nuclear reactions on target atoms. Over many years nuclear physicists have devised ways of accelerating particles to ever increasing energies. Now we have available beams of all nuclei from protons to uranium ions at energies well beyond those needed to study nuclear structure.

This apparently esoteric activity, driven purely by the desire to understand the fundamental forces governing the properties of atomic nuclei, has, along the way, produced a huge number of applications. Not only has it given birth to whole areas of science and supplied tools for many other kinds of science but it has, quite literally, changed our lives. Amongst its many progeny we can count reactor — and spallation — based neutron sources, synchrotron radiation sources, particle physics, materials modification by implantation, carbon dating and many other analytical techniques. Nuclear power, nuclear weapons, radiation therapy and non-invasive medical imaging are all things which derive from past research in nuclear physics and have altered our lives. Such studies have brought answers to many age-old questions including 'Why do the stars shine?', 'What heats the interior of the Earth?', 'How are the chemical elements made?', 'How old is the Earth?' and so on.

All of this grand edifice of knowledge and application has been built mainly on studies of nuclear reactions. Until now, however, nuclear physicists have had one hand tied behind their backs since the impressive achievements listed above have been realized through the acceleration of the 283 stable or long-lived nuclear species one can find here on Earth. These are exciting times for nuclear physicists because it has become evident that it is now possible to create and accelerate beams of unstable nuclei and there are $\sim 6000 - 7000$ distinct nuclear species which live long enough to be candidates for acceleration. It needs little imagination to see how this will transform not only nuclear physics but will lead to many new, undreamed of, opportunities in other areas of science.

In this article we will describe: the two main ways in which we can create beams of radioactive nuclei (section 2), our present knowledge of nuclear physics (section 3) and some of the obvious ways in which we can make use of beams of radioactive nuclei to study various areas of science (section 4).

2. The production of radioactive ion beams

Before launching into a discussion of how we might use beams of radioactive nuclei we should address the question: can we actually produce such beams other than by loading long-lived radioactive material into the ion source of a stable beam machine?

The answer is yes, we have found two generic ways of creating a range of radioactive ion beams, which are shown in schematic form in figure 1. They are known as the in-flight and isotope separator on-line (ISOL) techniques respectively. The two methods have been reviewed in detail in [1,2]. Here we outline their most important features.

Author's address: School of Physics and Chemistry, University of Surrey, Guildford, Surrey GU2 7XH, UK.

Contemporary Physics ISSN 0010-7514 print/ISSN 1366-5812 online
http://www.tandf.co.uk/journals
DOI: 10.1080/00107510110079233

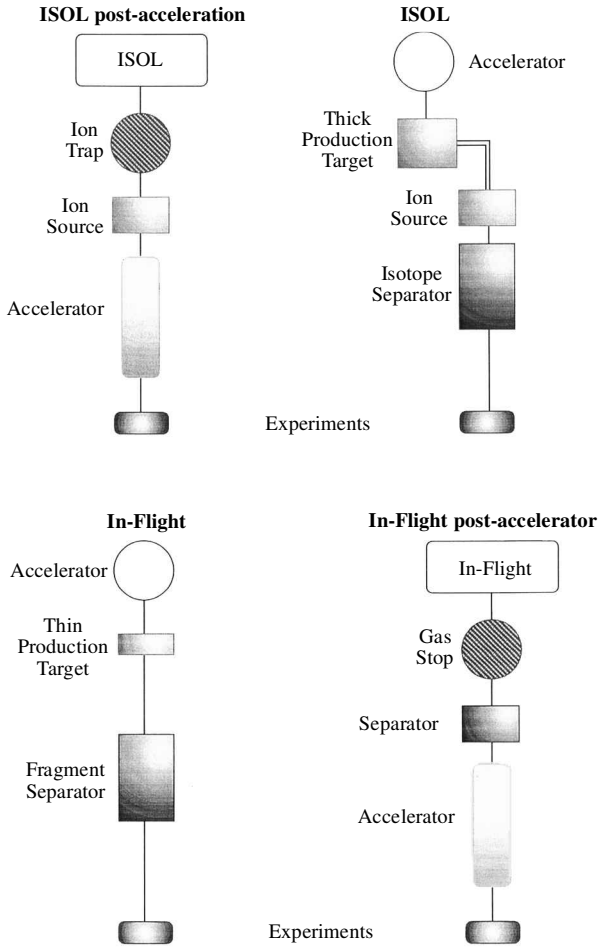

Figure 1. A schematic view of the basic methods of producing beams of radioactive nuclei. At the top we see the isotope separator on-line (ISOL) method with and without a post-accelerator. Below we see the in-flight method and the proposed hybrid in which fragments are caught in a gas cell and re-accelerated. [Courtesy of B. Jonson.]

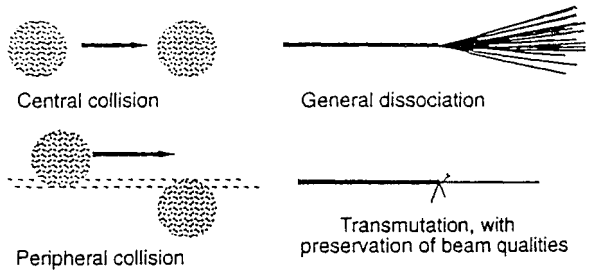

Figure 2. The figure gives a naïve view of central and peripheral collisions between two heavy nuclei at high energy. In the former the nuclei disintegrate into many small pieces. In the latter, part of the projectile is sheared off and the residue continues forward with the velocity of the projectile.

The most commonly used reaction with the in-flight method is high energy, projectile fragmentation. In essence the method is simple, provided one already has a beam of energetic heavy ions ($E/A \geq 30$ MeV u^{-1} and upwards). Figure 2 illustrates the process. If a central collision of the two heavy nuclei occurs at high energy the nucleus is shattered into many different, small pieces. The result is rather like the result of hitting a fly with a flyswat. This is not useful for our purpose. If the collision is peripheral, however, the effect is quite different. Here it is quite common to have the situation shown in the lower part of figure 2, where part of the projectile is sheared off but the remnant continues on in the forward direction with the beam velocity. In such a collision a range of different numbers of neutrons and protons can be exchanged. As a result the nuclei emerging from the target have different N/Z ratios both from each other and the projectile and take a range of values. Since the projectile fragments retain the velocity of the projectile they can be manipulated to form a beam which can be used for experiments.

What is produced is a cocktail of nuclei with various combinations of N and Z and atomic charge q. In general one cannot physically separate out the various species readily. Instead the fragments can be refocused and passed through a spectrometer such as the A1200 [3] at MSU or LISE3 [4] at GANIL. How does this work?

In passing the ions through a spectrometer such as LISE3 one can identify or tag them by A, Z and q from measurements of the $B\rho$ of the spectrometer magnets, time of flight through the spectrometer and energy loss in the final detector telescope. The spectrometer layout is shown schematically in figure 3. Measurements of the fields in the magnets combined with the position of an ion at the dispersive focal plane marked 2, measured with a position-sensitive, parallel-plate avalanche counter allow the determination of magnetic rigidity $B\rho$. At the final achromatic focus, a Si detector telescope is used to give two energy loss signals and a total energy signal. If we combine these measurements with the time of flight (TOF) from the first focal plane to the first element of the detector telescope, we have a unique measure of Z and A for each ion. Figure 4 shows an example of the results. The plot of ToF versus ΔE shows that the ions are clearly identified. Gamma rays or charged particles emitted in the subsequent interactions of the tagged ions are recorded in coincidence and are thus identified by the A and Z of the individual ions and associated with particular nuclear species. The gamma-ray spectra shown in figure 5 were recorded in just this way. This method works with the weak beams available at present. As beam intensities increase, more sophisticated methods of tagging or separation will be required.

This method is, in principle, easy to apply in laboratories where intense beams of high energy, heavy ions are already produced. There are four main centres for such research:

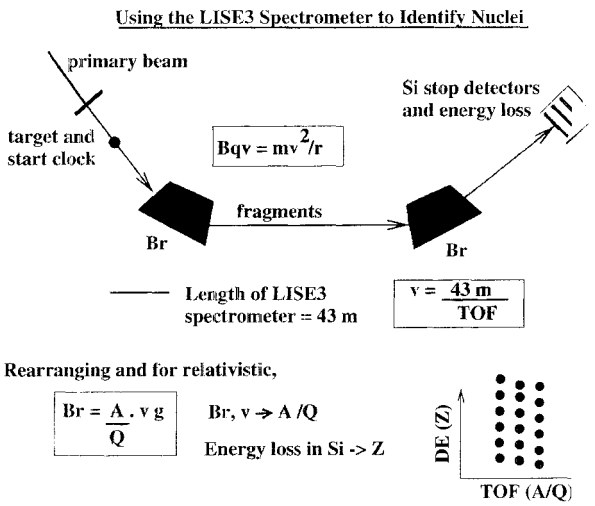

Figure 3. A schematic diagram of the layout of the LISE3 spectrometer [14] at GANIL. A cocktail of nuclear species produced in the fragmentation of a high energy, primary beam passes through the spectrometer. Measurements of the field strengths ($B\rho$) of the magnets, the time of flight (TOF) of the ions through the spectrometer and the energy loss (ΔE) in the final detector telescope allow one to identify each individual ion by A and Z.

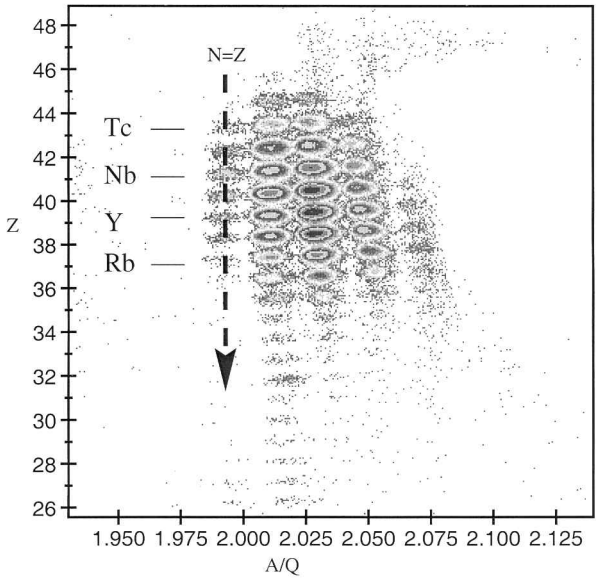

Figure 4. A two-dimensional identification plot of Z versus A/Q for ions produced in the fragmentation of 60 MeV u^{-1} ^{92}Mo ions on a natural nickel target at GANIL.

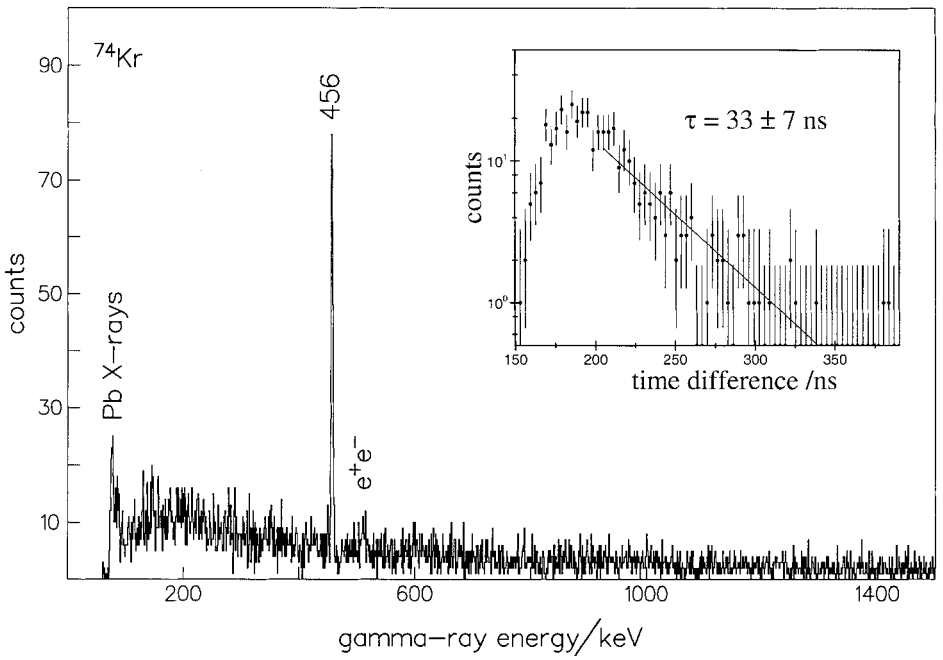

Figure 5. The spectrum of gamma rays in delayed coincidence with ^{74}Kr ions identified by A and Z in the plot shown in figure 4.

GANIL (France), RIKEN (Japan), MSU (USA) and GSI (Germany). Typically the primary beam energies are 30 – 100 MeV u^{-1} for the first three but are much higher ($\sim$1 GeV u^{-1}) at GSI. All four laboratories have been upgrading their capabilities and one can anticipate much more intense beams in the future.

One of the principal advantages of this method is that it is independent of the chemistry of the ions involved. Thus

all species long enough lived (typically >150 ns) to survive passage through the tagging spectrometer, can be produced and studied or used to initiate secondary reactions. Since they are produced at high energy there is also no need for post-acceleration, which means that one does not incur the costs of building a second accelerator. By their nature, however, such beams are poorly defined spatially and in terms of energy. They are also inherently weak and the intensities fall rapidly as we move away from stability (see figure 4). However, one would expect to see this method of production remain as the best method for beams of energy greater than ~ 30 MeV u^{-1}.

If the experiments require beam energies which are well below the optimal production energy in the in-flight method, it is possible to decelerate the secondary beam. It can be done by brute force simply by passing the beam through a thick degrader and this has been done in many cases. However the beam emittance grows so large that only a small fraction of the secondary beam is useful. In other words many of the particles are scattered out of the beam. To overcome this the beam has to be 'cooled' to maintain a reasonable secondary beam emittance during deceleration. At GSI a large storage ring has been built, called the ESR, which has just such capabilities. The effectiveness of cooling the radioactive ions was first demonstrated by Geissel *et al*. [5]. More recently the ESR has been modified [6] to include a stochastic cooling system. The ESR storage ring provides unique conditions for precision investigations in both atomic and nuclear physics. It has been used *inter alia* to test quantum electrodynamics by measuring [7] the 1s Lamb shift in H-like uranium, to measure [8] the masses and lifetimes of nuclear ground states and to study bound state beta-decay [9]. A summary of recent experiments with the ESR is given in [10].

There is a fundamental limitation to the process of beam cooling, namely the amount of time necessary to store and cool the ions, which is of the order of seconds. Thus ions with very short half-lives will decay during the process. In the deceleration process the intensities are reduced by one or two orders of magnitude due to limitations in the number of nuclei which can be cooled, space charge limitations, pulse structure matching and sometimes the time necessary for deceleration. Beam intensities lie in the range 10^6-10^7 ions per second or less. It should be noted that some of these difficulties would not be present for the weaker beams. Two rather more sophisticated storage rings have been proposed at JINR in Dubna [11] and RIKEN [12] in Japan.

In the ISOL or two-step method the modus operandi is quite different as illustrated in figure 1. Put simply, in the first step the radioactive species of interest are produced in reactions induced by a charged particle beam from an accelerator or by neutrons from a reactor. In principle any nuclear reaction can be used, whether it is induced by slow neutrons or high energy protons, provided it produces a sufficient number of the nuclei of interest. However they are produced, it will be in a thick target maintained at high temperature either by beam heating or by an external power source. At high temperature (~ 2500°C) the ions diffuse out of the target rapidly into an ion source. Once ionized in an ion source they can be extracted by an electric field, selected by A/q in a mass separator and then injected into a second post-accelerator which takes them to the energy needed in experiments.

In this method once we have created the radioactive nuclei of interest the accelerated beam is produced essentially in the same way as a stable beam, starting with ions in an ion source, so that the beam quality is similar to that in a normal accelerator. In other words one can manipulate the beam readily to give good spatial focusing, good energy resolution or good timing, whichever is appropriate for the purposes of experiment. This contrasts with the in-flight method. In principle there is no limit to the energy which can be reached in post-acceleration but it is constrained by cost and, since the in-flight method provides higher energy beams, it seems likely that in the near future the method will be restricted to a few tens of MeV u^{-1}. In contrast with the in-flight method the ISOL method is not equally effective for all chemical elements. Since the nuclei are produced in a thick target the release from the target and subsequent ionization in the ion source depend on the chemical nature of the element involved. For example it is no surprise, given their low ionization potentials, that alkali metals can be produced efficiently in abundance and it is difficult to extract refractory elements. Diffusion and effusion are involved in the passage of ions from the target to the ion source and they are relatively slow processes with time scales of milliseconds. As a result when we try to extract short-lived species we find that there are significant decay losses during this stage. Despite these difficulties it has been possible to produce low-energy beams of some 600 species involving 68 elements at CERN-ISOLDE [13].

This last bold statement does scant justice to an intensive target/ion source development programme at ISOLDE over some thirty years. ISOLDE shows clearly how well the ISOL method can work. In this case the driver accelerator is the CERN PS-Booster which provides $\sim 2\ \mu$A of 1.2 GeV protons to induce spallation in heavy targets. The extracted ions are then accelerated to ~ 60 keV for use in a variety of applications. More recently a room temperature linear accelerator (REX-ISOLDE) [14] is being added to allow acceleration to ~ 2 MeV u^{-1}.

A second example of a functioning ISOL system exists at Louvain-la-Neuve in Belgium. In this case a small cyclotron, which produces $\sim 200\ \mu$A of 30 MeV protons, is used to create radioactive species via (p, n) reactions. For example ^{13}N is produced in the form of ^{13}N^{14}N molecules

when the proton beam is used to bombard a graphite target enriched in ^{13}C. The nitrogen molecules pass into an ECR ion source where they dissociate and are ionized prior to injection into a $K = 100$ cyclotron. The latter acts as a high resolution mass spectrometer as well as accelerating the beam. This modest facility has been highly successful. The range of species produced is limited since it relies on 30 MeV protons to create them but useful beams of ^{6}He, ^{11}C, ^{13}N, ^{19}Ne and ^{35}Ar and other light nuclei are produced. The principal use has been to study reactions of astrophysical interest (see section 4.2). A new post-accelerator with 25% transmission producing ions with $0.2-0.8$ MeV u^{-1}, ideally suited to astrophysical reactions, will be in operation soon. This will produce beams with 10^{10} ions s^{-1} and further improve the isobaric separation. It will also extend the range of ions available since it releases the present accelerator to act as the driver. Its higher energy means that a greater variety of reactions can be used to produce the species of interest.

There is also a functioning ISOL facility at Oak Ridge National Laboratory in the USA based on a cyclotron plus Tandem Van de Graaff combination. It is the ideal tool for experiments which require good energy precision for their success (see figure 27 in section 4.3). It is not appropriate here to list the many other projects under consideration or construction around the world. The interested reader is referred to [15].

Recently US scientists have proposed a combination of the two methods, with which one might secure the advantages of the two techniques. It is also shown schematically in figure 1. Here the in-flight reaction products are slowed down by passage through a suitable material and then brought to rest in a gas cell, sucked out and separated by mass and then re-accelerated to the desired energy. In principle the method, advocated as the basis for the rare isotope accelerator (RIA) [16], should work. Indeed it has been shown to work with low efficiency in various IGISOL [17] systems, which operate in a similar way. If the method is successful it should produce radioactive species without chemical constraint and without the delays inherent in the ISOL process. However it will require considerable research and development to show that it is effective before one would hazard a large sum of money to build a facility based on it. Such research proceeds apace.

3. The present status of nuclear physics

Having established that we can produce beams of radioactive ions we can now turn to how we might use them to advantage (section 4) but it will help the reader if we first summarize our present knowledge of nuclear physics, since this is where the basic idea originated.

Atomic nuclei are not easy to study, in contrast to atoms and solids. In atoms, and hence in solids, the binding energies (eV – keV) are such that we can shine light or X-rays on them or bombard them with low energy electrons and learn about their structure by looking at how the radiation is diffracted or scattered or at the properties of the particles emitted by them under bombardment. We can also subject them to electric and magnetic fields or high pressure and again learn much about them. In contrast the binding energies in nuclei are of the order of many MeV not eV and we must have recourse to more dramatic and violent tactics to gain the information we desire about their structure.

In essence we can learn about nuclei from radioactive decay and nuclear reactions. We glean something from studies of radioactive decay, but it is a process which is essentially immutable for all practical purposes and we cannot control it. Our need, as in any area of physics, is to be able to vary the key parameters which describe the system, in this case the nucleus, in order to find how its properties vary. A humble analogy might be that we would never know that water can be a solid or a vapour if we were not able to change its temperature. In the same way, in studying nuclei, we would like to be able to vary, *inter alia*, the following key parameters; the temperature (E_{exc}, excitation energy), angular momentum (J) and the ratio of neutrons to protons $[(N-Z)/A]$. This key parameter space is illustrated in figure 6, which also attempts to show in cartoon form some of the things which happen to nuclei as these parameters are varied.

Exploring the space represented by this diagram relies on studying nuclear reactions. In the simplest of terms we simply make two nuclei collide and hence 'react'. We know their energies and velocities beforehand and we measure the energies and directions of motion of the resulting fragments and/or photons emitted. From these pieces of information we can then reconstruct the jigsaw to determine the properties of the nuclei involved in the collision. At any given bombarding energy in such collisions there are many possible end results and products. In essence anything which is energetically possible will occur although many of the processes will occur with such low probability that we can ignore them. Figure 7 gives a simplified view of just a few of the common outcomes of nuclear collisions.

Do they allow us to achieve our purpose of varying the key parameters? It is relatively easy to vary E_{exc} and J by altering the combination of target and projectile nuclei and the energy of the projectile. If we consider the latter our understanding of how nuclear properties vary with J has advanced rapidly since the early 1980s. The main tool has been the heavy ion induced fusion – evaporation reaction although one can also use Coulomb excitation and other reactions. The way the first of these proceeds is shown in figure 8. Once the two nuclei fuse to form a compound system it exists for a long time on a 'nuclear' time scale; usually taken to be the time for the projectile nucleus to

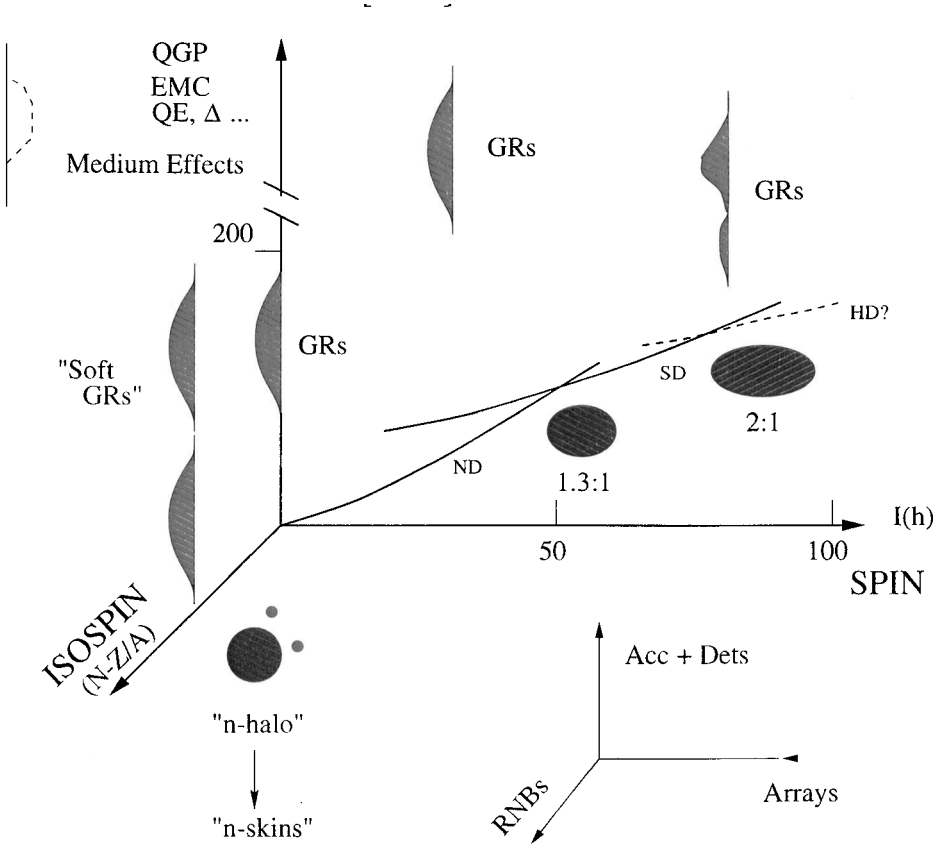

Figure 6. The diagram attempts to show the space defined by three key parameters describing the atomic nucleus. Studies of nuclear reactions allow one to vary these parameters, namely the excitation energy, angular momentum and the ratio of neutrons to protons. The various cartoons are intended to give an impression of some of the phenomena observed as the key parameters are varied. Most of these phenomena are mentioned in the text.

cross the nucleus i.e. $\sim 10^{-22}$ s. This compound system is 'hot', i.e. it is at high E_{exc}, and rotating rapidly. J can be as high as $50-80\hbar$, i.e. 10^{20} Hz. In essence we now have a hot, electrically charged, rapidly rotating liquid drop. Like any liquid drop it cools down by evaporating particles. These neutrons, protons and alpha particles carry away energy but not angular momentum. Following particle evaporation, the nucleus ends up cooler but still rotating very rapidly. The only way it can now lose energy is by emitting gamma-rays which carry away angular momentum. Thus a long cascade of 30–40 gamma-rays is emitted, leading through a series of excited states, to the ground state. In even–even nuclei the lowest states normally belong to a rotational band ($J^{\pi} = 0^+, 2^+, 4^+, 6^+ \ldots$) built on the ground state and the many possible cascades from the compound state usually funnel down into this ground state band or its equivalent in odd $-A$ nuclei. Studies of these gamma-rays reveal information about how nuclei react to rotation, i.e. how they are affected by the Coriolis force.

In practice our knowledge of the effects of rotation have advanced with improvements [18] in the arrays of Compton suppressed Ge detectors used to study the gamma-rays. In the ground state the nucleons are paired in time-reversed orbits. The Coriolis force acts to try to align the angular momenta associated with these pairs with the axis of rotation. As ω, the rotational frequency, increases this happens abruptly and we see a sudden change in angular momentum, a phenomenon known as backbending because of the characteristic shape of a plot of moment of inertia versus $\hbar\omega$. At high angular momentum it turns out that nuclei are particularly stable if they have a strongly deformed shape, like a rugby ball. These superdeformed nuclei [19] are in quantum states in a highly deformed mean field; the rugby ball has a 2:1 axis ratio. Theory suggests that hyperdeformed nuclei, with an axis ratio of 3:1, should also exist but they have not yet been observed.

Some of these phenomena, and similar effects revealed as E_{exc} increases, are shown as cartoons in figure 6. Although we have made much progress in exploring how nuclear

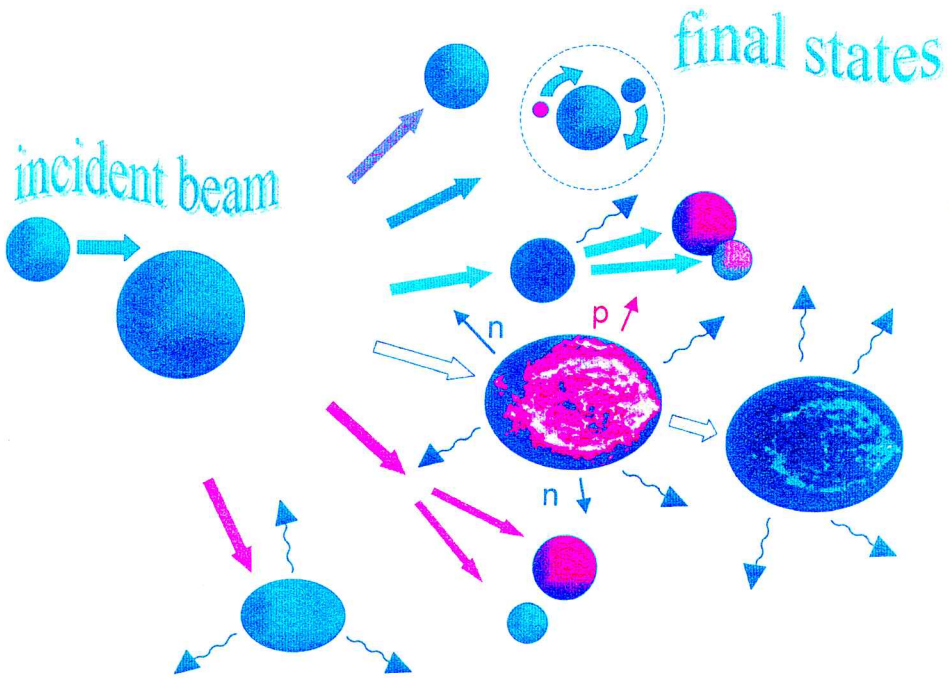

Figure 7. A simplified idea of some of the many types of reaction which may occur when two nuclei collide. [Courtesy of W. N. Catford.]

properties depend on E_{exc} and J we have made only limited headway in determining how they change with the balance in the ratio of neutrons and protons. The reason is not hard to find and is revealed in figure 9, which shows one version of the Chart of the Nuclides. Here the stable nuclei, shown as filled black squares, are plotted as a function of Z and N. Those unstable nuclei where we have some knowledge of their properties, even if it is only the mass or the half-life, are shown as unfilled squares. The continuous lines represent estimates of the so-called drip-lines, which connect the nuclei which are unstable to proton — or neutron — emission in the ground state; such nuclei cannot hold another proton or neutron if we try to add one. The name is meant to suggest the idea that if you add another neutron or proton it will simply 'drip' out again. If only stable nuclei are available as projectiles or target nuclei we are very limited in what we can study. We can reach nuclei outside a narrow strip around the line of stability with only a few types of reaction such as the fusion – evaporation reaction described earlier. As a result our detailed knowledge of nuclear properties is restricted to nuclei on or near the line of stability. In total there are 283 stable or long-lived nuclear species found in Nature. This compares with approximately 7000 species lying between the drip-lines. In principle most of these are long enough lived that if they can be created then they can be accelerated to an energy at which they could induce nuclear reactions. If this can be done in practice then it would make it possible to study all of the nuclear species on our chart (figure 9) in detail. It needs little imagination to see that this would transform nuclear physics and open the doorway to many other applications of nuclear physics. Our interest in producing beams of radioactive nuclei stems directly from the removal of this constraint; getting rid of the restriction to beams of stable nuclei.

4. The uses of radioactive beams

If history repeats itself, as it usually does, it is likely that the most exciting uses of beams of radioactive nuclei lie beyond our current imagining. Even without the benefit of a crystal ball, however, one can see a wide range of immediate uses in nuclear physics, nuclear astrophysics, condensed matter studies, bio-medicine, environmental measurements, etc. I do not intend to try to give here a detailed or exhaustive account of these possibilities. Instead I will give some examples in each area in order to give the reader the flavour of what we could hope to do if the relevant beams were available now.

4.1. *Nuclear physics*

4.1.1. *Neutron haloes.* If nuclear properties varied little with Z and N all of these fine words about creating and using beams of radioactive nuclei would count for naught in nuclear physics. One simple and dramatic example will

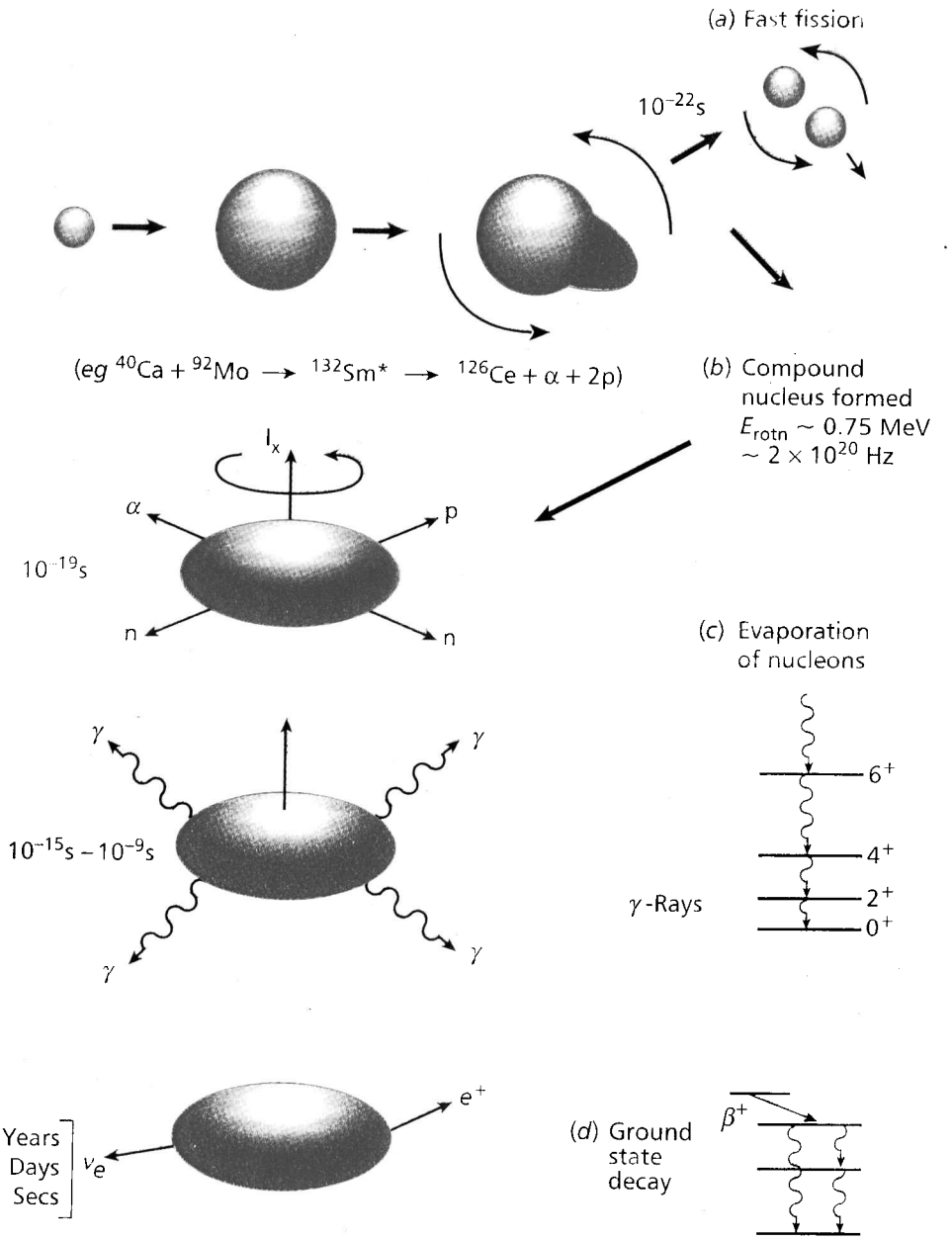

Figure 8. A schematic view of what happens in a fusion–evaporation reaction.

illustrate how different nuclear properties can be if N/Z is very different from the values encountered in stable nuclei.

The size or radius of the nucleus is one of the most easily understood and basic of its properties. Our knowledge of how large the nucleus is, stretches back to the beginnings of the subject and the experiments of Geiger and Marsden, which revealed the existence of the nucleus. A source of alpha particles (helium nuclei) was used to bombard a thin gold or copper foil. The transmitted alpha particles were detected by the fluorescence emitted when they impinged on a fluorescent screen. The expectation of the experimenters was that the alpha particles would be scattered at small angles but since they had been prudent and placed fluorescent screens at backward angles, to their surprise, an occasional particle was scattered backwards. Rutherford intepreted this in terms of scattering from the nuclear atom; a massive, positively charged central nucleus surrounded by electrons in orbit.

Inherent in this interpretation is a method of measuring the nuclear radius. As long as the scattering involves only electrostatic forces then the two nuclei are not 'touching', i.e. they do not feel the nuclear force. The distance of

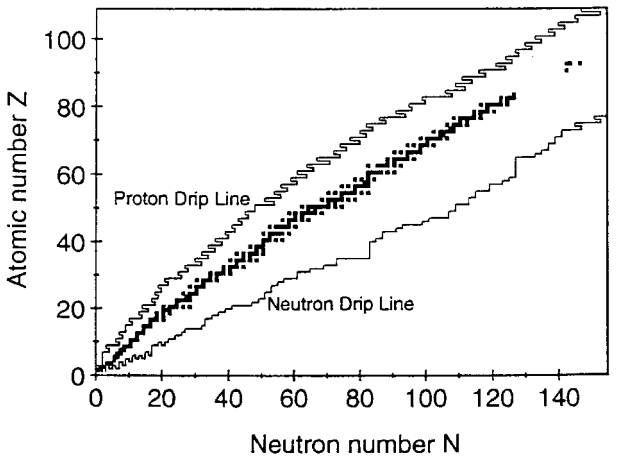

Figure 9. A simple version of the Chart of the Nuclides. The black squares represent the stable nuclei as a function of Z and N. Estimates of the proton and neutron drip-lines, the loci of points where we can no longer bind another proton or neutron, are shown as solid lines. Unstable nuclear species, where we have measured some property such as the mass or half-life, are shown as open squares.

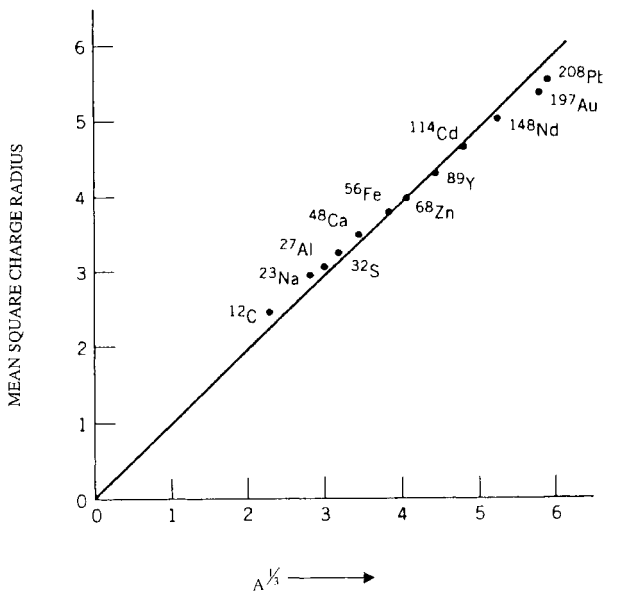

Figure 10. A plot of the root-mean-square charge radius for stable nuclei as a function of $A^{1/3}$.

closest approach is when the alpha particle is scattered backwards at 180°. In this case the initial kinetic energy of the alpha particle is turned into electrostatic potential energy at the point of closest approach (r_d). Thus,

$$\frac{1}{2}mV_\alpha^2 = \frac{2Z_1e^2}{4\pi\varepsilon_0 r_d}\,. \tag{1}$$

If we now increase V_α until this description breaks down we have reached the point where the two nuclei are just touching. We can then use equation (1) to give us a value for the nuclear radius.

In essence modern methods of measuring nuclear radii rely on the same idea. Now, however, we can use beams of high energy electrons, which do not feel the nuclear force. They have a very short wavelength and when they scatter from the nucleus they show a diffraction pattern which depends on the nuclear radius. If we see the electron in terms of a wave approaching an opaque disc, the nucleus, then it is just like the familiar optical diffraction pattern seen behind an opaque object. The detailed analysis is, of course, very similar to that describing the scattering of light. Over the years such experiments have been refined and measurements have been made of the radii of most stable nuclei. The results (figure 10) appear in many undergraduate textbooks and are taught to every physics undergraduate. Since the high energy electrons are essentially only sensitive to the protons, figure 10 shows the mean square charge radii for the nuclei concerned. Experiments with other projectiles, sensitive to the nuclear force, tell us that the neutrons and protons occupy the same volume. In other words the charge and matter radii are the same. As is obvious from figure 10 the principal result is summarized in the simple expression

$$R = R_0 A^{1/3}\,, \tag{2}$$

where R and R_0 are the nuclear radius and a constant ($\sim 1.2\times10^{-15}$ m) respectively and A is the number of nucleons in the nucleus ($A = N + Z$). In addition neutrons and protons occupy the same volume. Every undergraduate student in physics learns these two results.

All of this seems very clearcut. However in the last few years we have had available weak (10^3–10^4 pps) beams of some unstable, neutron-rich isotopes of light elements such as Li, Be etc. With these beams it is possible to measure the radii of the nuclei involved. At very high energy the total probability of interaction, i.e. interaction in any process, σ_I, when a nucleus passes through a target is given by

$$\sigma_I = \pi[R_I(P)^2 + R_I(T)^2] \tag{3}$$

where $R_I(P)$ and $R_I(T)$ are the radii of the projectile and target nuclei. This is because at high energies the interaction probability is essentially defined by the geometrical overlap of the projectile and target nuclei. Measurements with a single species of projectile on a series of targets will give a value for $R_I(P)$. The results for a series of Li isotopes are shown in figure 11. The results are roughly consistent with equation (2) until we reach ^{11}Li where there is a very big jump. It seems [20] that ^{11}Li has a radius consistent with that of a nucleus such as ^{48}Ca on the basis of equation (2).

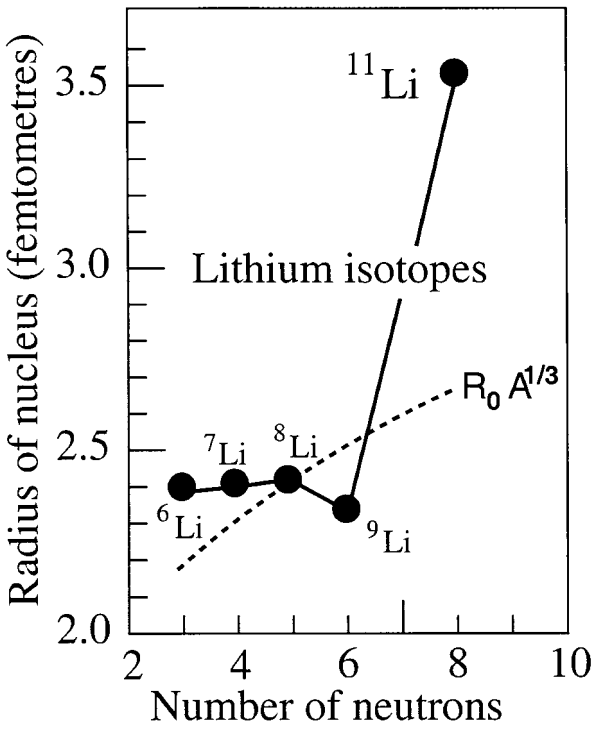

Figure 11. A plot of the root-mean-square charge radii of Li isotopes as a function of N (see text).

Related measurements shed light on this. Experimenters looked at the way ^{11}Li breaks up into ^{9}Li plus two neutrons in the nuclear or Coulomb field of another nucleus. They measured the distribution in momentum of the emitted neutrons, or in some experiments the momentum of the residual ^{9}Li particles. The measured spread in momentum (Δp) of these particles is directly related to the spread in their initial spatial distribution (Δx) in ^{11}Li by Heisenberg's uncertainty principle.

$$\Delta p \Delta x \sim \hbar . \tag{4}$$

If one measures the spread (Δp) for ^{9}Li particles at right angles to the beam there is a further complication because the spread is distorted by their subsequent deflection by other nuclei as they pass through the target. However measurements of the ^{9}Li momentum in the forward direction do not suffer from this problem since, by definition, they have not been deflected if they go straight forward. From measurements of this type one can deduce from the spread in linear momentum that in the initial state the neutrons extend well beyond the ^{9}Li core.

The results shown in figure 11 may then be interpreted in simple terms. The lighter Li isotopes conform to the rule of equation (2) but ^{11}Li is quite different, with a halo of neutrons extending well beyond the ^{9}Li core and giving the nucleus a size we might have expected for the much heavier ^{48}Ca.

Extensive studies have revealed a whole series of light, neutron-rich nuclei with haloes formed from one and two neutrons. Figure 12 summarizes the situation at the time of writing. A variety of models has been used to explain their properties. We can think of these models in terms of a quantum mechanical system in which neutrons and protons are bound together in a potential well. In stable nuclei the last proton or neutron lies quite deep in the well, bound by about 8 MeV. In halo nuclei the binding of the last neutron or neutrons is very much smaller. It does not take much energy to move the last, loosely bound neutron(s) a long way from the core. The uncertainty principle, in the form $\Delta E \Delta t \sim \hbar$, tells us that they can 'stay' there for a long time. Hence the neutrons in ^{11}Li can spread out in a 'cloud' around the core.

Thus in our very first excursion into unknown territory with beams of radioactive nuclei the results overthrow conventional wisdom. Accordingly we must modify our undergraduate textbooks and adjust our ideas.

4.1.2. *The limits of nuclear existence.* One of the simplest questions one might ask about atomic nuclei is 'what are the limits to the existence of nuclei?' It is a deceptively simple question and we do not have a definitive answer. Beams of radioactive nuclei will not necessarily supply the final answer but they will certainly take us very much closer to it.

There are three main frontiers in N and Z which define the limits of existence. A glance at figure 6 shows that there are, of course, limits in terms of other parameters as well. The frontier which attracts most public attention is the limit in Z. New chemical elements have always excited the imagination, which is not surprising given that our world is defined by the chemical elements. Our knowledge of the heaviest elements derives almost entirely from nuclear physics and the last few elements, or at least those we are sure of, have all been found at the GSI Laboratory in Germany.

4.1.3. *The heaviest elements.* Simple considerations suggest a natural termination to the existence of heavier chemical elements. Protons repel one another by the long-range Coulomb force and the nucleus is held together by the short-range nuclear force. As the number of protons increases we would expect it to become impossible to maintain the balance and nuclei would no longer hold together in the ground state. Even if we can put the requisite number of protons and neutrons together the nucleus will immediately fission. However about 25 years ago or so, it was realized [21] that there was another important factor which mitigated this effect.

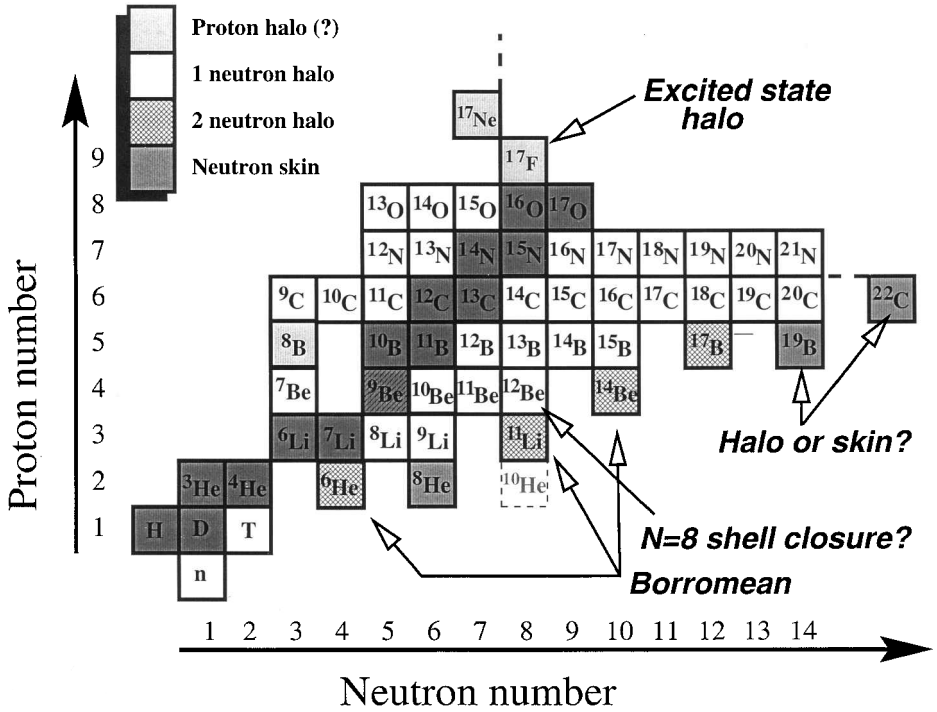

Figure 12. Part of the chart of the nuclides showing the light nuclei. It shows the nuclei which have been found to have one or two neutron haloes. The latter are Borromean systems; three-body systems which require all three components to be present to be stable. Here the three elements of the Borromean system are the core nucleus and the two attendant neutrons.

It is now well known that there is a shell structure in nuclei evocative of the familiar shell structure in atoms. It has its origins in the motion of the nucleons in a mean field created by all the other nucleons. The result is that for certain numbers of neutrons and/or protons there is an extra binding energy because a shell is complete. This extra binding gives the nucleus added stability. It manifests itself in stable nuclei in a number of ways. Nuclei with filled proton or neutron shells (Z, $N = 2$, 8, 20, 28, 40, 50 and 82, $N = 126$) appear in larger abundance in Nature, have larger separation energies for the last proton or neutron, etc. The initial prediction that this shell structure might lead to superheavy elements, stable even on a terrestrial time scale, has not been fulfilled but the idea itself has been confirmed by a whole series of experiments. The most convincing results so far have come from GSI where they have now identified [22] a few atoms of elements $Z = 110 - 112$. So far their attempts to create atoms with $Z = 113$ have been unsuccessful [23].

In essence the experiments are simple. The set-up is shown schematically in figure 13. A target consisting of heavy, neutron-rich nuclei, usually of ^{208}Pb or ^{209}Bi, is bombarded with a beam of neutron-rich projectiles such as ^{70}Zn. The bombarding energy is chosen so that when the two nuclei fuse together the compound system is relatively 'cold'. As a result there is then some probability that it will evaporate only a single neutron leaving a residual nucleus with $Z = Z_1 + Z_2$. The nuclei formed in these reactions recoil out of the thin target together with the non-interacting beam particles. A Wien filter system, consisting of crossed electric and magnetic fields, is then used to separate non-interacting beam particles and recoils. The recoils are then implanted into a Si detector. The pulse from the implanted recoiling ion starts the 'clock'. Energy and time signals from any subsequent alpha decay are also recorded. From these recorded signals one can then identify any correlated sequence of alpha particle decays. Any new species is then identified by the detection of an alpha particle of unknown energy, emitted shortly after implantation, followed by a sequence of alpha particles with the known energies and associated half-lives from the string of daughter nuclei, which have been measured in earlier experiments. The new species is firmly tied to the nuclei we already know by this chain of alpha decays. The correlation in time of the subsequent decays with the position and time of implantation and the characteristic energies of these decays together identify the new species.

This technique, so deceptively simple in concept and so difficult to put into practice, has been used by the GSI experimenters to create a few atoms of elements 110 – 112. Figures 14 and 15 summarize the situation. The former shows a particular calculation [24] of the extra energy

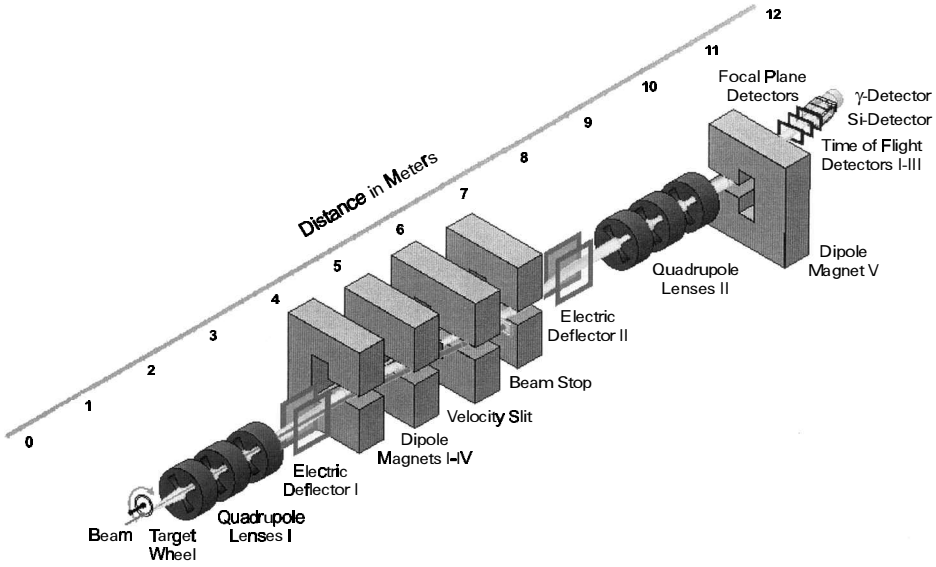

Figure 13. A schematic view of the SHIP separator at GSI which is used to separate superheavy nuclei produced in fusion–evaporation reactions from beam particles. [Courtesy of S. Hofmann.]

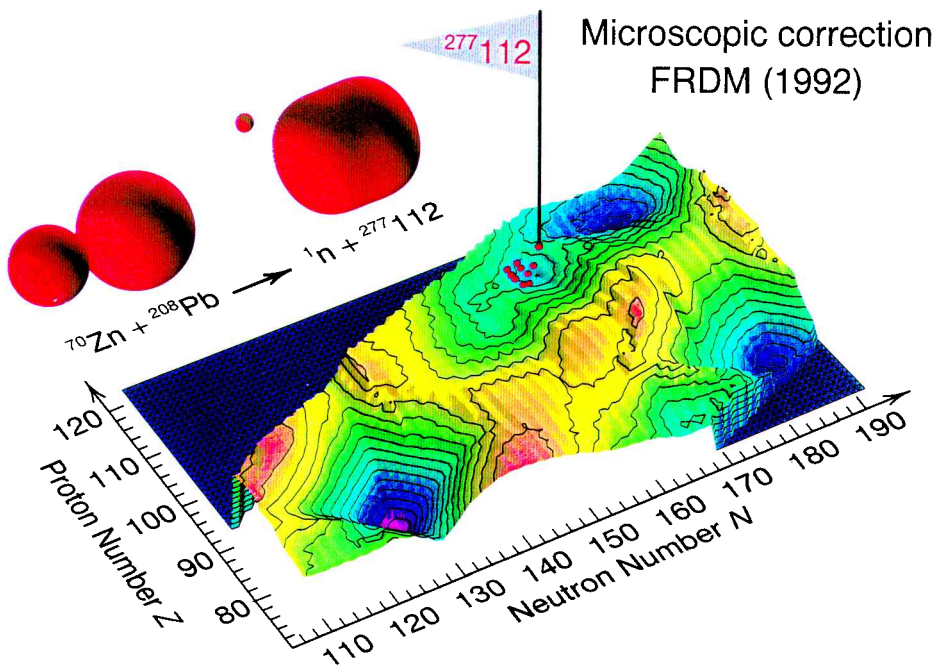

Figure 14. A plot of the calculated quantum shell correction as a function of Z and N. The valleys, increasingly blue in colour, indicate extra stability and hence indicate an undiscovered island of superheavy nuclei near $N = 184$. The red dots indicate nuclear species produced up to $Z = 112$ in fusion–evaporation reactions. [Courtesy of P. Møller.]

stabilizing the nucleus due to the effects of proton and neutron shells. We see that the calculation clearly indicates that ^{208}Pb ($Z = 82$, $N = 126$) is particularly stable, which is consistent with all the known properties of this, the heaviest, stable, doubly magic nucleus. The picture also shows two other regions of particular stability in heavier nuclei. The red dots show us the nuclear species which have been made over recent years culminating in the implanted flag marking element 112. Figure 15 summarizes the increasing difficulty of reaching heavier elements in this

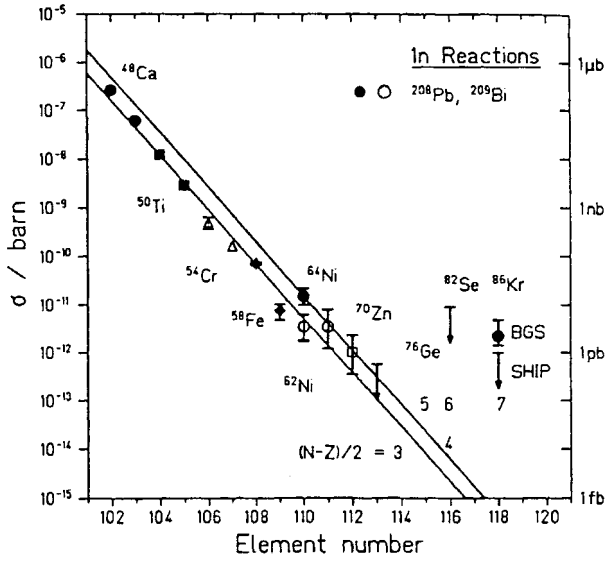

Figure 15. A plot of measured cross-sections for the production of heavy elements in cold fusion reactions [22, 23]. The points for element numbers 116 and 118 show recent results. The point marked BGS was reported by Ninov *et al.* [26] and that marked SHIP shows an upper limit on the same cross-section.

way. It shows, on a logarithmic scale, the measured cross-section (in simple terms the probability) for creating the nucleus of interest as a function of Z. Overall the trend is that the cross-section drops by a factor of 3 for each step in Z.

Over the last 18 months or so, however, we suddenly have reports of the possible observation of heavier elements still. Prompted by new calculations by Smolanczuk [25], who predicted a value of 670 pb for the $^{86}\mathrm{Kr} + {}^{208}\mathrm{Pb} \rightarrow {}^{293}118 + 1\mathrm{n}$ reaction (cf. a value of $\sim$fb suggested by figure 15), this reaction was studied by Ninov *et al.* [26] at Berkeley with a new gas-filled recoil separator (BGS) as the recoil/beam particle selection device. In essence the predicted 3–4 orders of magnitude increase in cross-section over the trend seen in figure 15 comes from the fact that ^{86}Kr has a closed neutron shell. In the experiment three events with the same apparent alpha decay chains were measured and assigned to the decay of ^{293}118. The measured cross-section is shown in figure 15 together with a subsequent attempt to repeat the experiment at GSI which could only set an upper limit to the cross-section. To date the Berkeley result remains unconfirmed.

In addition exciting new results have been reported [27] from Dubna where a different philosophy is followed. The experiments described above rely on 'cold' fusion with quite low excitation energy (temperature) in the residual nucleus formed in the fusion of the projectile and target nuclei and the evaporation of a single neutron. At Dubna hot fusion experiments have been carried out with long-lived radioactive ^{242}Pu, ^{244}Pu and ^{248}Cm targets bombarded with intense beams (~ 0.7 pμA) of the neutron-rich species ^{48}Ca. Typically, in these experiments, the compound nucleus is formed with an excitation energy of 30–36 MeV with the consequence that it will de-excite most probably with the evaporation of 3–4 neutrons and gamma rays. Technically the experimental set-up is similar in concept to the GSI experiments although the spectrometer used to separate the recoils of interest from scattered beam particles, etc. is gas-filled in this case. The Dubna experiments led to the observation of several short decay chains which were associated with the decay of isotopes of elements 112 and 114 and, more recently, a single decay chain associated with the decay of an isotope of element 116 with mass 292 which feeds into ^{288}114 seen earlier. Figure 16 shows the details of the decay chain observed as well as of the two events observed earlier and associated with element 114 and mass 288. All of these decay chains end in spontaneous fission. Although the results are not confirmed by experiments elsewhere as yet, they do appear to be internally consistent.

Figure 17 is an attempt to summarize all of this. It shows the centre of the predicted 'island of stability' on the right and the various decay chains observed in the experiments described above. Three points should be noted. First whereas the decay chains observed at GSI for elements up to 112 link with known nuclear species, those from the experiments at Berkeley and Dubna do not, which makes confirmation of the results more problematic. However, as mentioned earlier, the Dubna results appear to be internally self-consistent. Secondly for elements 112 and 114 the observed half-lives do increase as we move towards neutron-rich nuclei. This is consistent with the approach to the most stable, predicted species. Thirdly in terms of the predictions overall the nuclei which are observed to fission are predicted to do so.

Where do radioactive ion beams come in? The answer also lies in figure 15. Here we note that when one uses ^{64}Ni instead of ^{62}Ni, and more generally $T_Z(=(N-Z)/2)$ rather than $T_Z = 3$ nuclei, as the projectiles then the fusion reaction probability increases. There are some grounds then for believing that if we could produce radioactive ion beams with large T_Z we can not only create systems closer to the centre of the 'island' but the cross-section would also be larger. The reader should note that this pre-supposes beams comparable in intensity to those currently available with stable beams. This will not be easy to achieve but it is a glittering prize!

Superheavy elements, quite apart from their intrinsic interest, are important because they will allow critical tests of nuclear models, in terms of their predictions of both structure and stability, of relativistic effects in atoms and of quantum chemistry. At present 'real' chemistry [28] has reached element 106. Once we understand the reaction

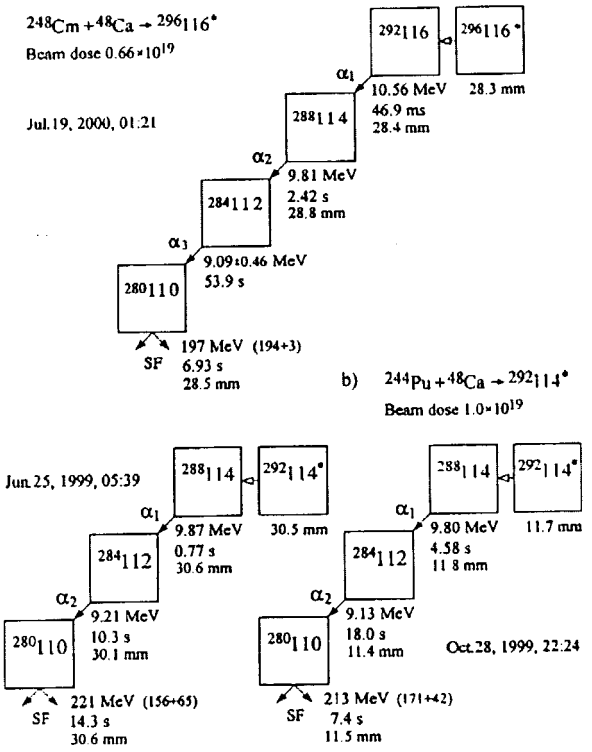

Figure 16. The figure shows details of the alpha-decay chains from element 116 reported recently from Dubna [27] together with decay chains seen earlier from the isotope of $Z = 114$ to which it decays.

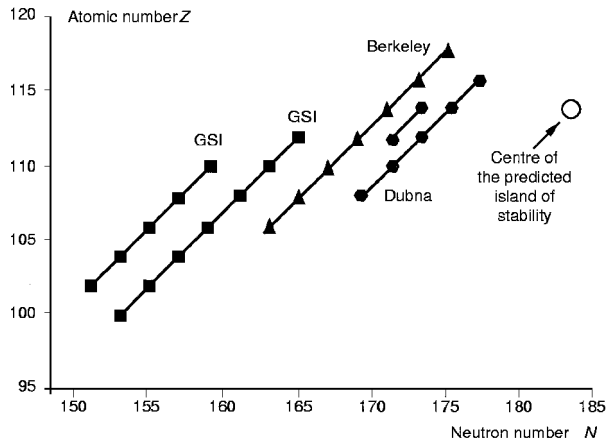

Figure 17. The figure shows alpha-decay chains reported in experiments aimed at producing the heaviest nuclear species. On the right we see the predicted centre of the island of stability for superheavy elements at $Z = 114$, $N = 184$. The diamonds denote nuclear species observed [22] in the alpha decay of elements produced at GSI. The triangles denote the reported [26] alpha-decay chain for element 118. The octagons represent the nuclear species reported [27] from experiments at Dubna. The right-hand chain, starting with the alpha decay of $^{292}116$, feeds $^{288}114$. This species was produced independently and decays by the same alpha chain. It should be noted that the decay chains observed at Dubna end in spontaneous fission.

mechanisms involved in the production of the heaviest elements, we can hope to extend the chemistry studies considerably.

4.1.4. *The proton drip-line.* The proton drip-line is the dividing line between nuclei which are bound and unbound with respect to proton emission from their ground states. In other words as we add protons it is the point where the nuclear ground state becomes unstable. For the lightest elements, the nuclei beyond the drip-line are only seen fleetingly as resonances in reaction cross-sections. However as Z increases this situation changes because of the increasing Coulomb barrier faced by the proton. This is illustrated in figure 18 where we see the proton faced by a barrier which depends on both the Coulomb force and the amount of angular momentum carried away in the decay. From this simple picture it is clear that proton decay occurs by quantum mechanical tunnelling in just the way alpha decay occurs. As in alpha decay the rate of decay depends on the width of the barrier. Clearly proton decay may not be observed exactly at the point where the drip-line is reached because the barrier is too high. If we are to see proton radioactivity it must have a significant decay branch which may mean that we are several isotopes beyond the drip-line. As figure 18 shows the width of the quantum mechanical barrier depends on the angular momentum carried away. As a result the tunnelling probability and hence the half-life is very sensitive to the orbital angular momentum of the emitted proton. From the measured proton-decay energy and half-life one can deduce the angular momentum transferred in the process and hence determine the ordering of the proton shells beyond the drip-line; an invaluable test of theoretical models of nuclei far from stability.

Figure 19 shows the proton emitters which have been observed above $Z \sim 50$ where the Coulomb barrier is large enough for the phenomenon of ground state proton radioactivity to occur. These results effectively map out much of the drip-line above $Z = 50$.

Below ^{100}Sn ($Z = 50$) the drip-line is being defined by studies of fragmentation reactions. As described in section 2 the products of such reactions can be identified by A, Z and q by passing them through a spectrometer such as LISE3 [4]. Such a system allows one to test whether any particular species lives long enough to survive the transit time of ~ 0.5 μs through the spectrometer. In an experiment [29] typical of this type, the very neutron-deficient nuclei $^{77}_{39}$Y, $^{79}_{40}$Zr and $^{83}_{42}$Mo were all identified for the first time but no evidence was found for the existence of $^{81}_{41}$Nb and $^{85}_{43}$Tc. The nuclei were produced in the fragmentation of ~ 100 enA of 60 MeV u^{-1} ^{92}Mo ions on natural Ni targets of thickness $50 - 100$ mg cm^{-2}. The reaction products passed through the LISE3 spectrometer and stopped in a four element Si detector telescope. Figure 20 shows the identification plot of Z versus A/Z for the ions surviving transit. It also shows,

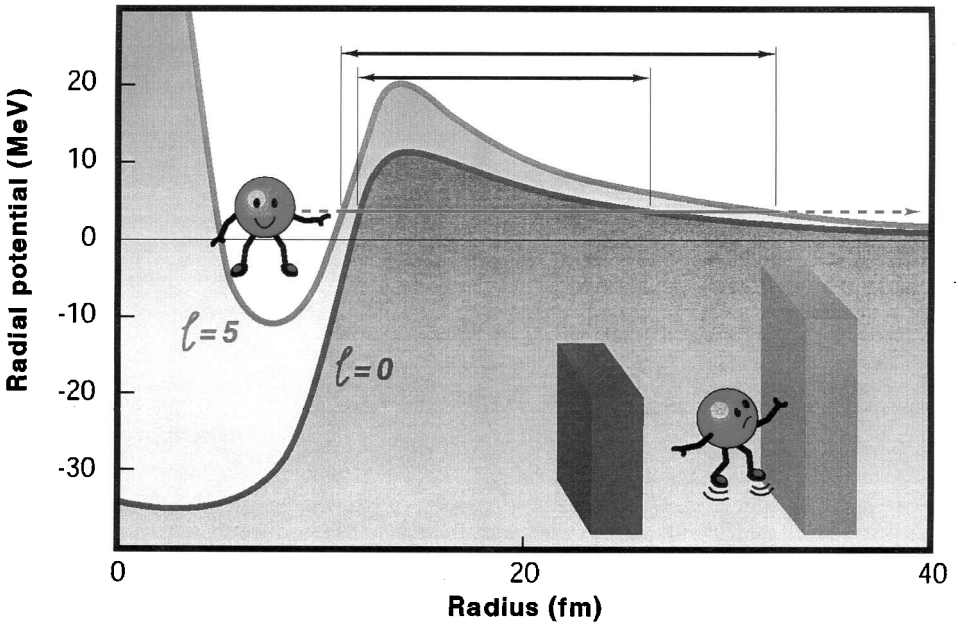

Figure 18. A light-hearted view of how ground state proton decay results from quantum mechanical tunnelling through a barrier created by the Coulomb and centrifugal forces. The half-life of the decay is highly sensitive to the width and height of the barrier and hence to the angular momentum (*l*) carried away by the proton.

on the right-hand side, projections of this plot for $T_Z = 0$ and $T_Z = -1/2$, where $T_Z = (N-Z)/2$. The latter clearly shows the presence of ^{77}Y, ^{79}Zr and ^{83}Mo as well as the previously known ^{75}Sr. From these measurements one can also set limits of 80 and 100 ns for the half-lives of ^{81}Nb and ^{85}Tc respectively. Although not conclusive it is likely that these two nuclei are proton unbound.

The observation of ^{77}Y is perhaps surprising given the instability [30,31] of the $Z = N + 1$ systems ^{69}Br, ^{73}Rb, ^{81}Nb and ^{85}Tc. Janas *et al*. [29] explain this in terms of the extra stability produced by the highly deformed, prolate $Z = N = 38$ core.

In terms of the mapping of the proton drip-line, experiments of this type tell us clearly whether a particular nuclear species lives long enough to survive transit through the spectrometer. The absence of a given species in plots such as that shown in figure 20 is a strong indicator that it is unbound. It turns out that this information is often important for nuclear astrophysics as well.

For $Z < 21$ the Coulomb barrier is low and no proton-unbound nuclei have been directly observed in this region. However systems which are proton-unbound, such as ^{12}O, ^{15}F, ^{16}Ne and ^{19}Na have been studied in direct reactions, such as (^{3}He, ^{8}Li) [32], (^{4}He, ^{8}He) [33] and (π^+, π^-) [34]. Although the nuclei involved can only exist as short-lived resonances, one can detect the stable ejectile and the kinetics of the two-body system allow one to determine the ground-state mass and excited states of the unstable system.

Overall, as the above summary indicates we have a good idea of where the proton drip-line lies. Once good quality beams of radioactive nuclear species are available we should be able to study the nuclei up to and part of the way beyond the proton drip-line.

4.1.5. *The neutron drip-line.* The situation with regard to the neutron drip-line is very different. Apart from the very lightest nuclei (see figure 12) the bounds of neutron stability are quite unknown experimentally. The reasons are two-fold. Since there is no equivalent of the Coulomb barrier the neutron drip-line lies much farther away from stability and our attempts to create the nuclei still fall well short of the drip-line.

One might well ask whether there is a neutron drip-line. After all we believe that we observe neutron stars, which we could picture as gigantic atomic nuclei. However gravity plays a very large role in stabilizing the neutron star, a role which is absent in normal nuclei. As figure 12 shows we have reached the drip-line in the lightest nuclei. However these nuclei are so small that their properties are dictated by surface effects and hence this does not settle the question.

Myers [35] has considered the question seriously and presents convincing arguments that the drip-line exists, in line with our simple expectations. He considered whether neutron matter is stable within the framework of a Thomas–Fermi model of nuclei and looked at the consequences of bound or slightly unbound neutron

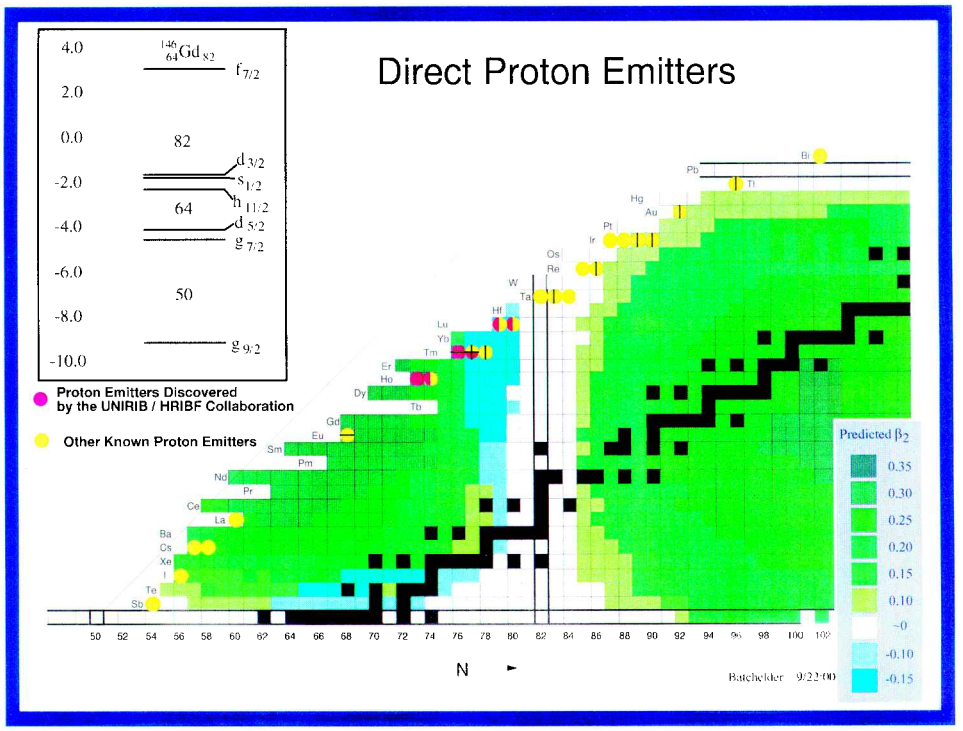

Figure 19. A plot showing the ground state proton emitters which have been observed in experiments. The inset on the right shows the colour coding for the predicted quadrupole deformation (β_2) of the nucleus, i.e. how much the nuclear 'rugby ball' deviates from the spherical shape. The inset on the upper left shows the sequence of single particle levels for the nucleus ^{146}Gd. [Courtesy of J. Batchelder.]

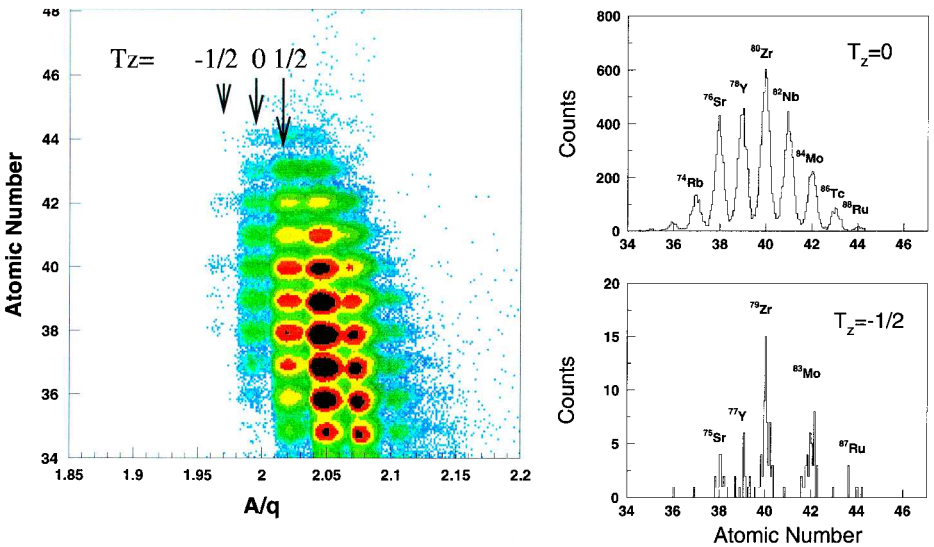

Figure 20. Two-dimensional plot of atomic number Z versus mass-to-charge ratio A/Z to identify nuclei produced in the fragmentation of ^{92}Mo ions at 60 MeV u^{-1}. The right-hand side shows projections of this particle identification plot on to the Z axis for the $T_Z = 0$ and $T_Z = -1/2$ nuclei. Note the presence of ^{77}Y, ^{79}Zr and ^{83}Mo.

matter. If neutron matter were unbound, nuclei could exist in quite exotic structures such as neutron balls of arbitrary size. They could contain clusters of protons, with a variety of topologies, held apart by the Coulomb repulsion. Myers compared the results of his Thomas – Fermi calculations with the observed drip-line in the lightest nuclei. Even allowing for the dominant surface effects in such small nuclei Myers concluded that 'neutron matter is probably not bound' but that one might expect effects such as neutron haloes (see section 4.1.1). Myers' arguments are convincing but do not tell us where the drip-line is.

For predictions of where the neutron drip-line lies we must turn to semi-empirical formulae for nuclear masses and binding energies. Loosely speaking these are based on the idea of the nucleus as a charged liquid drop. The various versions of these models involve a variety of approximations and parameters with both the theoretical techniques and parameters optimized to reproduce the known atomic masses of nuclei near stability. As a result, for any given version one has little idea whether it reproduces the variation of mass with particle number with any accuracy when we move to extreme N/Z ratios.

One can see this clearly in figure 21 which shows the predictions of the masses of the tin ($Z = 50$) isotopes as a function of mass number. Not surprisingly the various models fit the masses well on and near stability but diverge rapidly as we move away from the known masses of the nuclei near stability. As a result if we use them to predict the location of the neutron drip-line we find that the predictions differ by 20 – 30 neutrons in the case of tin.

Two developments will alter this. First the development of radioactive ion beams has meant a rapid advance into the *terra incognita* of exotic nuclei on both sides of stability. Amongst the most spectacular of these forays are the discoveries of ^{100}Sn [36], ^{78}Ni [37] and ^{48}Ni [38], which hold out the promise of access to a wider range of exotic nuclei. Secondly there have been rapid advances in methods of measuring masses [39]. In particular the spectacular improvements in ion traps have meant that one can store and manipulate small numbers of ions thus allowing the determination of their masses. It is also possible to retain ions in storage rings such as the ESR at GSI (see section 2), which we can think of as a very large ion trap. Figure 22 shows the mass spectrum of ^{143}Sm ions held in the GSI storage ring and one can see that the ground state and isomeric state at 754 keV are clearly separated. This gives a clear impression of just how well we can measure masses if we can create the ions and get them into the trap/storage ring.

These developments will undoubtedly lead to a much better knowledge of nuclear masses. The result will be much improved predictions of the masses of neutron-rich nuclei and hence of the location of the drip-line.

4.1.6. *Shell structure far from stability.* One of the most striking features of nuclei near stability is the shell structure. This is, of course, a very familiar phenomenon in atoms, where the central Coulomb potential in which the electrons move leads to particularly tightly bound structures for the noble gases He, Ne, Ar, Kr, Xe. Intuitively one would not expect the same thing to happen in nuclei where there is no central object and the interactions between the individual nucleons is very strong. Accordingly one would not expect nucleonic orbits to persist because the nucleons

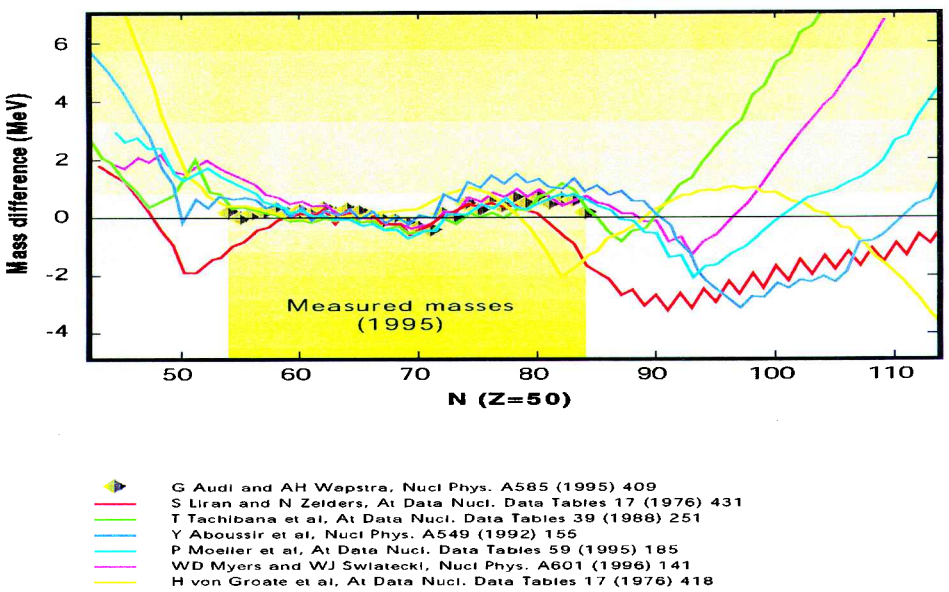

Figure 21. The measured binding energies of tin isotopes compared with the predictions of various semi-empirical formulae.

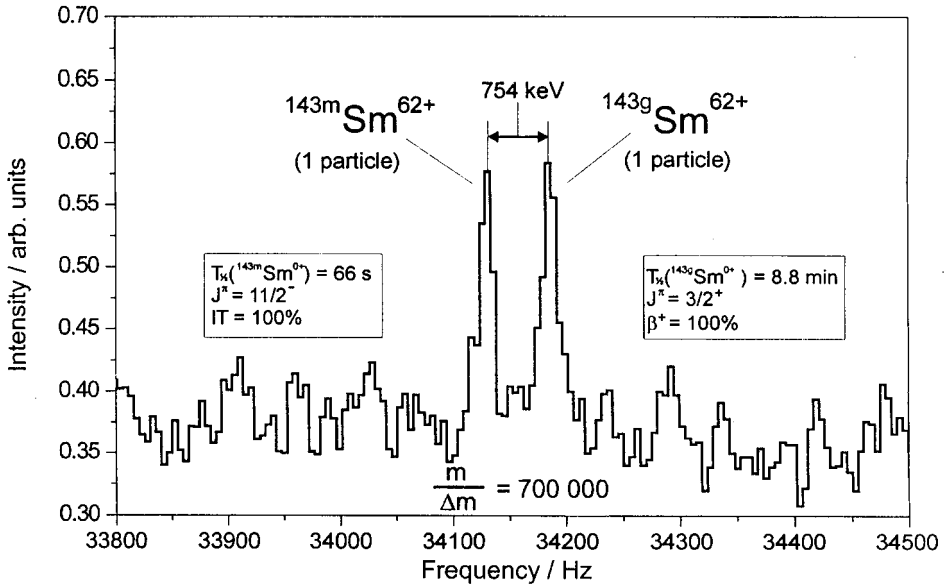

Figure 22. The Schottky spectrum of ions stored in the ESR storage ring. It shows clearly the signals from individual ions in the ground state and isomeric state at 754 keV in ^{143}Sm.

would be scattered immediately they encounter another nucleon. However all of the experimental evidence is that certain values of Z and N, the so-called magic numbers, lead to particular stability. The answer to the conundrum is simple in the end. The nucleons move in the mean field due to all the other nucleons and this plays the role of the central potential. At the same time the Pauli principle prevents scattering into orbits already occupied. As a result the orbits do persist.

On the right-hand side of figure 23 we see the ordering of the single particle orbits for heavy elements and one can see clearly the pronounced gaps at the magic numbers 50, 82 and 126. This can be reproduced theoretically with an effective NN (nucleon – nucleon) interaction and a spin – orbit (l.s) interaction. Within this picture we have a good idea of the structure of single-particle states, collective modes and global properties of nuclei near stability. However if we consider nuclei with extreme N/Z ratios we have no real clue about the shell structure because we do not know how the NN interaction varies with the changing isospin.

This question has been considered by Dobacewski and co-workers [40] and reviewed by Dobacewski and Nazarewicz [41]. In some sense figure 23 summarizes their conclusions. Their results suggest that near the drip-line the shell structure is dramatically affected by coupling to the particle continuum because the outer nucleons are so loosely bound. The large diffuseness of the neutron density and central potential leads to a single-particle spectrum in neutron drip-line nuclei which resembles that of a harmonic oscillator with a spin – orbit term. As figure 23 shows even

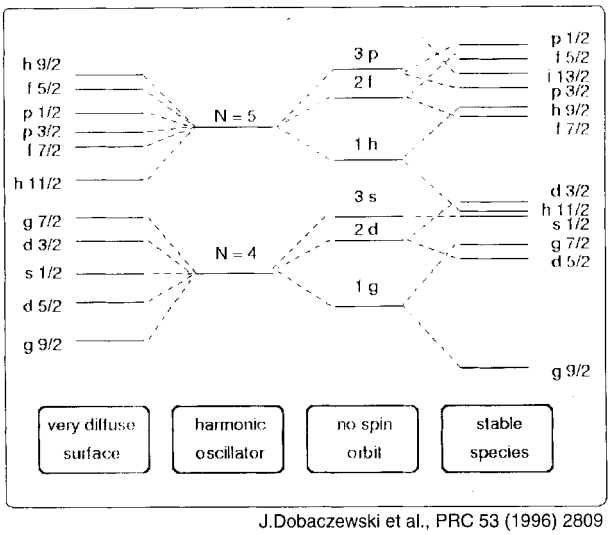

Figure 23. On the right we see the sequence of single particle levels for stable and near-stable nuclei. It is determined empirically by adding l.s and l^2 terms to a Woods – Saxon potential. To the left we see what happens if there is no spin – orbit (l.s) term or just a simple harmonic oscillator or what may happen if the nucleus has a very diffuse surface.

the pronounced shell gap at $N = 82$, seen in proton-rich and stable nuclei, effectively disappears as we approach the drip-line.

If correct, these changes would have profound effects on nuclear properties and nucleosynthesis via the r-process (see section 4.2) which proceeds via many nuclei in this regime. So what is the reality? Without beams of radio-

active ions to allow us to reach neutron-rich nuclei it is difficult to test these predictions. However, even with the beams we have there is evidence that shell structure is different far from stability. For example N and $Z = 40$ are clearly sub-shells in stable nuclei but in a series of experiments [42] it was shown that ^{80}Zr, with $N = Z = 40$, far from being spherical as one expects for a closed shell nucleus, is amongst the most deformed of nuclei in its ground state. Thus the idea that the shell structure is not immutable as N/Z changes is already firmly established. As indicated earlier (section 3) the positions of the shell gaps also depend on the rate of rotation of the nucleus, another of our key parameters.

Among the simple signatures of the closed shell in even Z, even N nuclei is the high excitation energy of the first excited 2^+ state and the corresponding weakness of the transition de-exciting this state to the ground state. Both these quantities can be measured simultaneously if one can produce a beam of the relevant nuclei and measure the energies and intensities of the gamma rays emitted following their excitation by the Coulomb force when they impinge on a target. The gamma-ray spectra from ^{66}Ni and ^{68}Ni ions, produced in projectile fragmentation (see section 2), Coulomb excited by a lead target at the end of the LISE3 [4] spectrometer, have been studied at GANIL. The resulting excitation probabilities for the Ni isotopes ($Z = 28$) as a function of N are shown in figure 24. This provides clear evidence of the weakening of the $N = 40$ subshell in neutron-rich nuclei. It will take much systematic study with a wide range of radioactive ions to explore fully the shell structure far from stability.

The change in shell structure also means that unusual combinations of orbitals will come close to the Fermi surface. Collective excitations, which involve the coherent motion of a large number of nucleons, are sensitive to such changes. Indeed one may expect entirely new forms of collective motion. In near-stable nuclei we are already aware of modes of excitation in which the proton and neutron distributions oscillate against each other. If we now have another component involved, namely the neutron halo or skin, it is possible to have oscillations of this skin against the core. Such excitations will only be found with intense beams of neutron-rich radioactive nuclei. The experimental signatures relate to the characteristics of the gamma rays associated with their decay. Their identification would signal the presence and the extent of the neutron skin.

We have only scratched the surface of this topic. The predicted changes in the shell structure with N/Z will bring many changes which cannot all be anticipated. Their discovery awaits the availability of suitable beams of radioactive ions.

4.2. *Nuclear astrophysics*

Nowhere is the success of nuclear physics so evident as in its application to astrophysics. The formation of hydrogen and helium and a pinch of other light species in the Big Bang, the generation of energy in stars, the creation of the elements up to Ni/Fe in fusion reactions in main sequence stars and the creation of heavier elements in the s- and r-processes are all, in principle, explained by nuclear physics. Amongst its particular successes is the interpretation of the observed galactic isotopic abundance distributions in terms of both primordial and stellar nucleosynthesis [43].

Despite these successes we have taken only the first steps towards understanding these processes. Rapid advances in observational techniques, involving not only the study of the entire electromagnetic spectrum but the proliferation of space-based observations free from atmospheric interference and absorption, have produced a veritable cornucopia of new information about abundance distributions in the winds of massive stars and the ejecta of novae and supernovae and also about galactic gamma-ray sources. This information links the production of a range of chemical elements and nuclear species with particular astrophysical sites. It also provides the key to our understanding of both nucleosynthesis and energy generation at these sites. If we are to benefit from this bounty we need two things. First we need increasingly sophisticated models

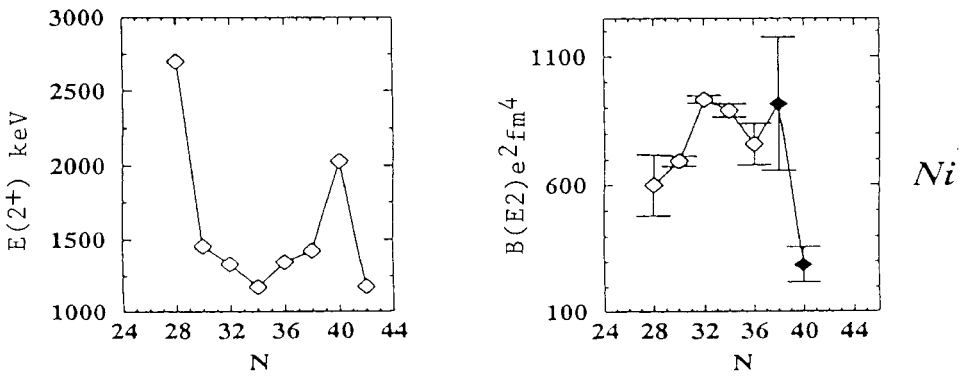

Figure 24. The energies and de-excitation transition probabilities of the first excited states of the even Ni isotopes.

of stellar hydrodynamics in dealing with explosive events driven by nuclear processes. The rapid advances we have seen in computing power make this possible. Secondly we need a detailed knowledge and understanding of the nuclear physics which lies behind all this. It turns out that to obtain this requires a wide range of radioactive ion beams. Without them and the results to be obtained with them, interpreting the information the astronomers have worked so hard to provide will not be possible.

The reasons are straightforward. Nucleosynthesis and energy generation are just two faces of the same coin. Both depend on the time scales of nuclear reactions and radioactive decays, which in turn depend critically on the physical conditions of temperature, pressure, etc. In Main Sequence stars things proceed sedately but when the end comes, when explosive conditions set in, it is very different. Now the time scales shorten dramatically. In the conditions in Main Sequence stars radioactive decay rates are comparable to reaction rates. At the elevated temperatures and pressures in explosive conditions the huge increase in nuclear reaction rates means that they dominate whilst these conditions last.

It is not appropriate here to recount the whole story of nucleosynthesis; instead our readers are referred to [44,45] for the detail and we will summarize only the salient points. Figure 25 shows a version of the Chart of the Nuclides which shows some of the important points. The story starts with fusion reactions in Main Sequence stars. Beginning with the primordial materials, H and He, the products of the Big Bang, we get the successive burning of H then He then C and O and so on up to Fe/Ni, where the process stops because fusion reactions no longer release energy but, instead, require energy to make them happen. Along the way the elements up to Fe/Ni are created. Of course, this is dangerously simplistic. In stars like the Sun we believe the process stops at C, N and O. The central temperature is too low for burning to go further; the reactions involving heavier nuclei are then too slow for the process to continue. Again in massive stars it is not simply a matter of burning successively heavier species, a process reminiscent of an addict squandering his/her assets on one last fix. Instead, once a high enough temperature is reached there is a sufficient flux of gamma rays that there is a constant flow back and forward between (γ,p) and (p,γ) reactions. Gradually, however, there is a drift to heavier elements and the continuation of burning heavier elements in fusion reactions. In massive stars the end is abrupt. Since fusion cannot continue beyond Fe/Ni, because energy is no longer

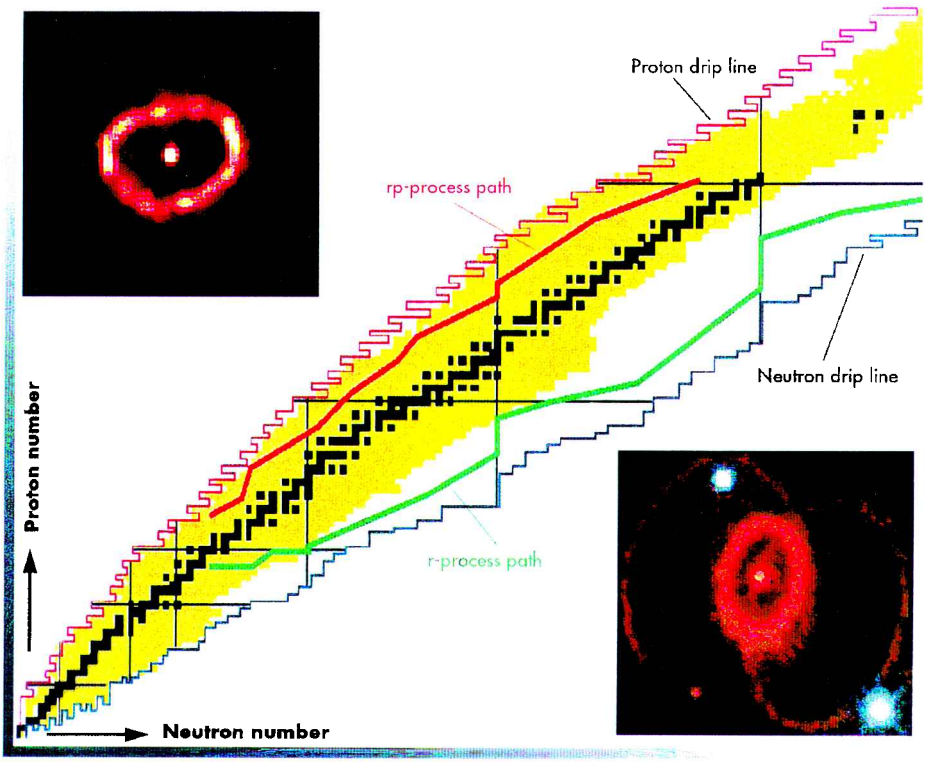

Figure 25. Chart of the nuclides showing the limits of present observations, the drip-lines and the astrophysical r- and rp-process pathways. The insets show Hubble Space Telescope images of the nova CYGNI 1992, a possible site for the rp-process and the afterglow of SN1987A, an r-process site.

released in the reaction, the star is no longer stable and collapses in a spectacular supernova. In a brief span of time there is a huge outpouring of neutrons, photons, neutrinos, etc. In the high neutron flux, starting with a given isotope we can get a long series of neutron captures, with capture occurring so rapidly there is no time for beta decay. Finally when the neutron flux dies away the very neutron-rich nuclei which have been created decay back to the line of stability. The feedstock, the nuclei we started with, are transformed into heavier elements. This process is known as the r-process (rapid neutron capture process). The reaction pathway it follows is shown in figure 25. This may not be the only route to the creation of the heaviest elements. Colliding neutron stars would also provide an environment in which the equivalent of the r-process might occur.

A somewhat similar process, involving nuclei on the other side of the line of stability, occurs in other explosive environments such as novae and X-ray bursts. A typical nova is thought to involve a binary system composed of a massive red giant star and a white dwarf. Material (mostly hydrogen) from the Red Giant is pulled by gravity on to the surface of the white dwarf which is rich in C, N and O. The accumulated material forms a thin but dense envelope at the surface which mixes with the C, N and O dredged up from the material of the white dwarf. The temperature and pressure at the bottom of this surface layer steadily builds up. The details [46] of what happens next depend on the mass of the white dwarf and how rapidly it accumulates material but, crudely speaking, it is as follows. In essence thermonuclear ignition occurs once the temperature and pressure are high enough. It occurs under conditions in which the electron gas is degenerate, which leads to a very rapid increase in temperature at constant pressure and density. The result is 'thermonuclear runaway'. This is further enhanced by the presence of the ^{12}C, ^{14}N and ^{16}O nuclei from the white dwarf, which act as catalysts for the hot CNO cycle (see below). Because the temperature in the burning shell on the surface rises very rapidly, the peak temperature rises above the Fermi temperature before the electron gas is non-degenerate enough to start expansion. Convection means that energy is transported rapidly to the surface ($\sim 10^2$ s). The positron emitters formed in the hot CNO cycles are also carried to the surface and release their decay energy. The result is a violent burst of energy and material ejected from the star.

How does nucleosynthesis proceed in such an environment? Figure 26 shows the classic CNO cycle which plays a role in energy production in some Main Sequence stars. At $T \sim 2 \times 10^7$ K, reaction and beta decay rates are similar and we get a sequence of proton captures and beta decays the result of which is

$$4\mathrm{p} \rightarrow {}^4\mathrm{He} + 2\mathrm{e}^+ + 2\nu + 24.69\ \mathrm{MeV} \qquad (5)$$

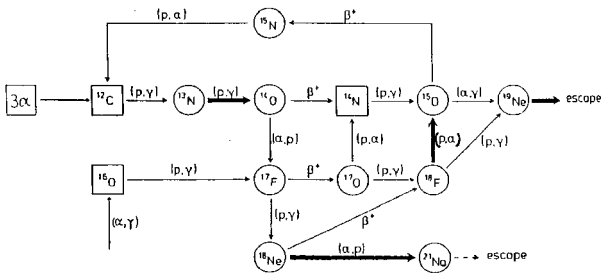

Figure 26. The figure shows the network of nuclear reactions and beta decays involved in the CNO reaction cycle in stars.

with the C, N and O nuclei acting simply as catalysts. However at $\sim 5 \times 10^8$ K, a typical nova temperature, the reaction rates are much more rapid. Now ^{12}C (p,γ) ^{13}N is followed not by beta decay but by ^{13}N (p, γ). Instead of a closed cycle a rapid series of reactions leads to a rapid breakout from the CNO cycle with the production of heavier nuclei. This leads, in a very short time, to a series of proton captures all the way up to close to ^{100}Sn. Much work [47] has been done on this rp-process (rapid proton capture) in recent years. The likely path of this rp-process is shown in figure 25.

The striking feature of both the r- and rp-processes is that they involve radioactive species. The reaction pathway associated with the former involves neutron-rich nuclei far from stability. The rp-process pathway lies close to the $N = Z$ line and the proton drip-line. In both cases the nuclei are difficult to access and study with beams of stable nuclei. Their common feature is that they involve reactions on unstable nuclei. The only way to study these reactions is to generate beams of the unstable species and study their interactions with targets of H, He, etc., i.e. they have to be studied in inverse reactions with a heavy nucleus incident on a light target nucleus.

In principle one needs a vast amount of information on many nuclei. However not all of it carries equal weight [48] in terms of calculating the resulting elemental abundances so that the number of key experiments is finite. Nevertheless there is much to be done if we are to interpret the astronomical observations. Even with the limited range of beams available now this process has begun. They are the harbingers of much more to come. Here a few examples must suffice.

The first successful experiment with an ISOL beam (see section 2) certainly attacked a key experiment. From figure 26 we see that the ^{13}N (p, γ) ^{14}O reaction rate is critical to break out from the CNO cycle. A direct measurement was reported by Decrock *et al.* [49] using a beam of $\sim 3 \times 10^8$ pps of ^{13}N. Proton capture on ^{13}N is expected to populate the state at 5.17 MeV excitation energy in ^{14}O. In essence the experiment was simple. The 5.17 MeV gamma rays de-exciting this level were detected

with a Ge detector and the number of ^{13}N ions incident on the target measured. The result for the width of this state, $\gamma = 3.8$ (1.2) eV, agrees with the other indirect measures of the cross-section. This experiment is important not only because of the importance of this cross-section but also because it was the forerunner of a wide range of important nuclear astrophysics experiments to come. It should be noted that this particular case is unusual in that the cross-section is large enough to be measured in this simple, direct manner. Much more typical is the case of ^{19}Ne (p, γ) ^{20}Na where Page *et al.* [50] have attempted to measure the cross-section in an indirect way because it is smaller by orders of magnitude.

Many other reactions are important in the breakout from the CNO cycle. As we see in figure 26 the nucleus ^{17}F plays a role in stellar explosions via several reactions, including the ^{17}F(p,γ)^{18}Ne reaction. Indeed it is thought [46] that in the ignition phase of X-ray bursts the production of energy peaks via two reaction sequences: ^{12}C(p, γ)^{13}N(p, γ)^{14}O and ^{16}O(p, γ)^{17}F(p, γ)^{18}Ne(e^+, ν_e) ^{18}F(p,α)^{15}O. In this second reaction sequence the production of energy in the X-ray burst depends sensitively on the ^{17}F(p,γ)^{18}Ne reaction cross-section. Again in massive stars, in the pre-supernova phase, the temperature in the Ne shell can rise to $1-2\times10^9$ K. The result is that ^{16}O can burn to form ^{17}F which, if the (p, γ) cross-section is large enough, may then undergo burning. If one is to understand the elemental abundances produced in such events it is clear that one must know the ^{17}F(p, γ)^{18}Ne stellar reaction rate.

In this case one would hope to be able to calculate the reaction rate reasonably well from our knowledge of the structure of ^{18}Ne. Wiescher *et al.* [51] looked at this problem and concluded that the reaction rate should be dominated by a low energy 3^+ state in ^{18}Ne, the mirror to the known 3^+ state at 5.378 MeV excitation energy in ^{18}O, for temperatures above 0.2×10^9 K which is within the range of peak temperatures produced in these explosive events. They predicted that the 3^+ state in ^{18}Ne should lie at 4.328 MeV and have a width $\Gamma \approx \Gamma_p = 5$ keV. A range of other estimates followed [52]. The fly in the ointment was that no such state had been seen in earlier experimental studies involving the ^{16}O(^{3}H, n)^{18}Ne and ^{20}Ne(p, t)^{18}Ne reactions. However these reactions favour the population of states with natural spin and parity.

Recently it has become possible [53] to produce weak beams ($\sim10^4$ pps) of radioactive F isotopes from the HRIBF facility [54] at Oak Ridge. Since the post-accelerator involved is a 25 MV Van de Graaff, which produces a beam with precise energy control and good energy resolution, the facility is ideally suited to look for resonances in reaction cross-sections. In this case, Bardayan *et al.* [55] sought evidence for the 3^+ state in ^{18}Ne as a resonance in the ^{1}H(^{17}F, p)^{17}F excitation function. The details of the experiment, which involved the bombardment

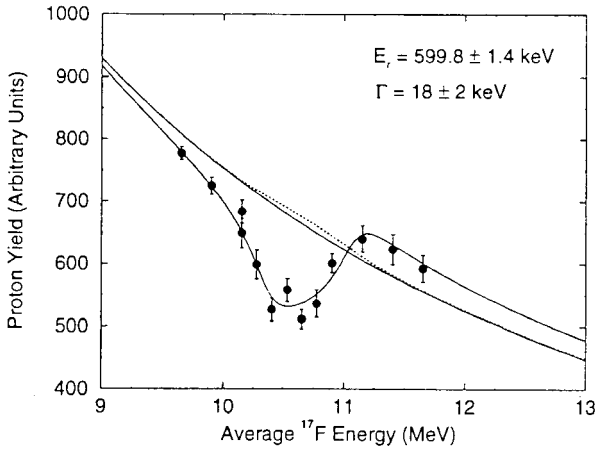

Figure 27. The figure shows the excitation function [55] in the ^{17}F (p,p)^{17}F reaction. The resonance observed defines the width and energy of the 3^+ state in ^{18}Ne populated in the ^{17}F (p, γ)^{18}Ne reaction (see text).

of a thin (48 μg cm^{-2}) polypropylene target with the ^{17}F beam and the detection of the ^{17}F recoils in coincidence with the scattered protons, can be found in [55]. The resulting excitation function is shown in figure 27. Here we see the normalized proton yields as a function of average ^{17}F beam energy in the target. The fit to the data involves the normalization, resonance energy and width of the 3^+ state. The other curves show the expected excitation function if the 3^+ state did not exist and the only resonances were the previously observed 1^- and 0^+ states in ^{18}Ne. The results clearly reveal the 3^+ state at 4519(8) keV excitation energy with a width of $\Gamma = 18(2)$ keV.

This result confirms that the 3^+ state contributes strongly to the ^{17}F(p, γ)^{18}Ne stellar reaction rate above 0.5×10^9 K and is thus very important in explosive events such as X-ray bursts and supernovae.

One topic of considerable interest is the endpoint of the rp-process. The nuclei with $N\sim Z$ play a crucial role in hydrogen burning on the surface of accreting neutron stars in X-ray binaries. They are special because from mass 50–100 the $N=Z$ line for odd Z is thought to coincide with the proton drop-line and, therefore, with the path of the rp-process. Beyond $A\sim70$ our knowledge of the reaction and decay processes for nuclei along the rp-process path is very limited indeed because of the very small cross-sections for producing these nuclei in fusion–evaporation reactions. Indeed, since they are very close to the drip-line, it is not clear *a priori* that the nuclei are particle stable. If not, this may result in the termination of the rp-process at that point. A number of other nuclei have long beta decay half-lives so they may also effectively end the process. However it has been shown that the

effective lifetime may be much shorter because of two sequential proton captures bridging the gap. Two proton captures can also bridge the unbound isotopes ^{69}Br [48] and ^{73}Rb [49].

In section 4.1.2 it was explained how we can determine whether nuclei near the proton drop-line are particle stable or not. Figure 20 shows the nuclear species formed in the fragmentation of 60 MeV u^{-1} ^{92}Mo ions on thick, natural Ni targets. Janas *et al*. [29] showed that ^{77}Y, ^{79}Zr and ^{83}Mo are particle stable. At the same time it appears that ^{81}Nb and ^{85}Tc are particle unbound. Thus experimental studies of fragmentation products are beginning to shed light on the rp-process pathway.

As stated earlier these are only a few examples of the flood of results to be expected once beams of radioactive nuclei become more widely available. We can look forward then to a much better understanding of the energy dynamics and the conditions prevailing in explosive events in stars.

4.3. *Materials science*

Materials science has benefited in many ways from the application of nuclear physics. Amongst the benefits is the use of accelerators to implant ions into materials to manipulate and alter their properties. The method allows one considerable control in placing a known number of dopant atoms at a chosen depth in a material. It is clean and selective and allows the use of any combination of stable beams and materials. The process is also free of the normal solubility or alloying rules of chemistry. It allows one to modify the mechanical, chemical, electrical, magnetic and optical properties of materials. All in all it is a powerful tool.

It has been used *inter alia* to create a wide range of semiconductor devices with properties tailored to specific applications and to create machine tools and replacement parts, such as artificial hips [54], for the human body which are particularly tough or wear resistant.

Where do radioactive ions come into this story? The answer is straightforward. Ideally we would want to know in detail where the implanted stable ions end up in these materials. We would like to know about their local, microscopic environment. We would like to know what sort of lattice sites they occupy in crystalline materials for example. Such information might then allow us to refine the technique in terms of creating better and novel devices. If a radioisotope of the same chemical element as the implanted ions exists, with suitable decay characteristics, then one can form a beam with exactly the same characteristics as the stable beam and implant the radioactive ions into the material. By measuring how the decay characteristics of the unstable species are altered we can deduce the nature of their environment.

4.3.1. *Radioactive spies.*

In a sense we can think of the implanted radioactive nuclei as spies reporting on the local environment in the host material. Figure 28 illustrates this with an implanted atom sitting close to a lattice site in a crystal lattice. In this position it interacts with neighbouring atoms and information concerning this interaction is then communicated to the outside world by changes in the pattern of its radioactive decay. Various techniques, including perturbed angular correlations (PAC), Mössbauer spectroscopy and the emission channelling of conversion electrons, alpha particles and positive or negative beta particles fall into this category. Some examples of their use follow.

Hydrogen is one of the most important impurities in semiconductors from both the scientific and technical points of view. During various steps in the manufacture of semiconductor devices it is easily incorporated into the semiconducting material, where it interacts very efficiently with other impurities or defects. It saturates dangling bonds, passivates shallow and deep-level dopants or impurities, or causes new, hydrogen-related electronic levels. Its behaviour is complicated, since it can appear as H^+ or H^- or in neutral form or as a stable or metastable molecule or in precipitation, and this makes it difficult to understand the formation of complexes and hydrogen diffusion.

In the hydrogen passivation of donors or acceptors we have the formation of next-nearest, electrically inactive, hydrogen-dopant pairs. Due to the Coulomb interaction H^+ (H^-) ions are trapped at the ionized acceptors A^- (donors D^+). The resulting complexes are electronically neutral and inactive and, hence, the resistivity of the semiconductor increases. The free migration of well-defined H configurations in III – V semiconductors, such as InP or GaAs, can be studied on an atomic scale using the PAC technique with the probe atom ^{117}Cd → ^{117}In, which is populated in ^{117}Ag decay. One starts by irradiating the sample with a clean ^{117}Ag beam. The sample is then annealed to remove damage and loaded with H^+. The Coulomb interaction between ionized acceptors (Cd^-) and donors (H^+) induces the formation of Cd – H pairs. Following the decay of ^{117}Cd the pair is transformed to In – H, and since the H^+ no longer feels the attractive Coulomb force it is able to migrate. The onset of migration can then be observed by PAC. Figure 29 shows the measured time-dependent coincidence ratios for PAC measurements on a series of hydrogen-passivated III – V semiconductors together with the corresponding Fourier transforms [56]. Well-defined electric field gradients (EFG) were observed in all the materials. In GaP and InSb only one EFG was found but in GaAs, InAs and InP up to two different EFGs, corresponding to two different H-induced complexes, were found. All the EFG tensors are axially symmetric and the main axis is orientated in the ⟨III⟩ lattice

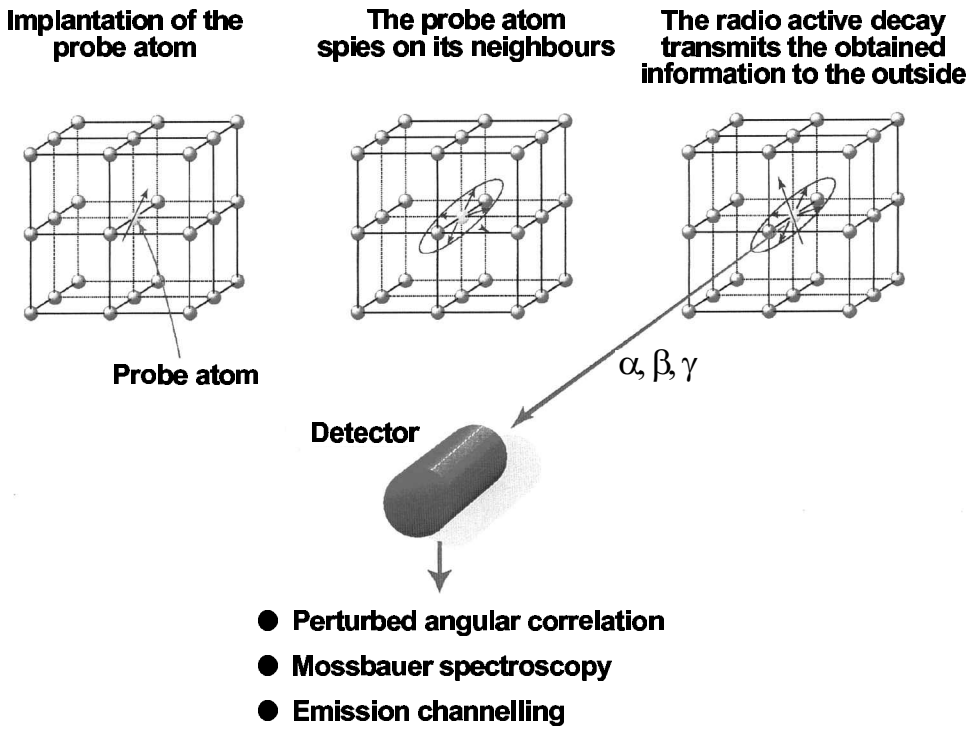

Figure 28. Ions implanted in semiconductors and other materials can act as 'spies' on the microscopic environment they end up in. These properties are probed by the way in which the radiation emitted in the subsequent radioactive decay is modified. A variety of techniques can be used for this purpose.

location. PAC experiments not only inform us of the nature of the microscopic structure of complexes but also how stable they are if measurements are made as part of an isochronal furnace annealing programme.

Detailed information about the microscopic environment of implanted atoms can also be gleaned from the channelling of conversion electrons (see e.g. [57]), beta particles or alphas. Mössbauer spectroscopy allows the same thing.

Until now the use of Mössbauer spectroscopy has been limited because it relies on the existence of pairs of nuclei such as ^{57}Fe/^{57}Co where a low-energy Mössbauer state in a stable isotope is fed in the decay of a long-lived parent which can be conveniently produced, purified and incorporated in a suitable matrix. The technique provides detailed chemical and structural information on the environment at the Mössbauer nucleus. If the radioactive atom can be implanted, the requirement for a long half-life is removed and one can identify a large number of candidate Mössbauer systems, totalling some 75 cases distributed over 40 elements. Some examples, chosen at random, include ^{67}Zn/^{67}Ga, ^{161}Dy/^{161}Ho and ^{197}Au/^{197}Pt. The parent nuclei would be produced as radioactive beams, thus allowing convenient implantation into the sample of interest. This and all the other techniques will benefit from a wider range of species from ISOL facilities (see below) and, indeed, their use will spread when more such facilities exist.

4.3.2. *Curing chemical blindness.* In many techniques used to study solids one obtains spectroscopic signals which originate in particular chemical elements but there is nothing in the measurement which reveals which element is involved. The use of implanted radioactive ions allows one to overcome this difficulty and effectively cure the chemical blindness of the technique. Thus in the last decade a range of conventional semiconductor physics methods such as deep level transient spectroscopy (DLTS), capacitance voltage (CV), Hall effect (HE), photoluminescence spectroscopy (PL) or electron paramagnetic resonance (EPR) has been combined with the use of radioactive isotopes. The chemical transmutation of the dopant in radioactive decay provides a clear chemical fingerprint. The intensity of the observed electrical or optical signals changes with the characteristic time constant of the radioactive decay and allows one to assign electrical or optical properties to a particular chemical element unambiguously.

Most of the electrical properties of semiconductors are determined by the bandgap states of impurity defects or atoms. Such levels are frequently detected and characterized by spectroscopic techniques that reveal their electronic

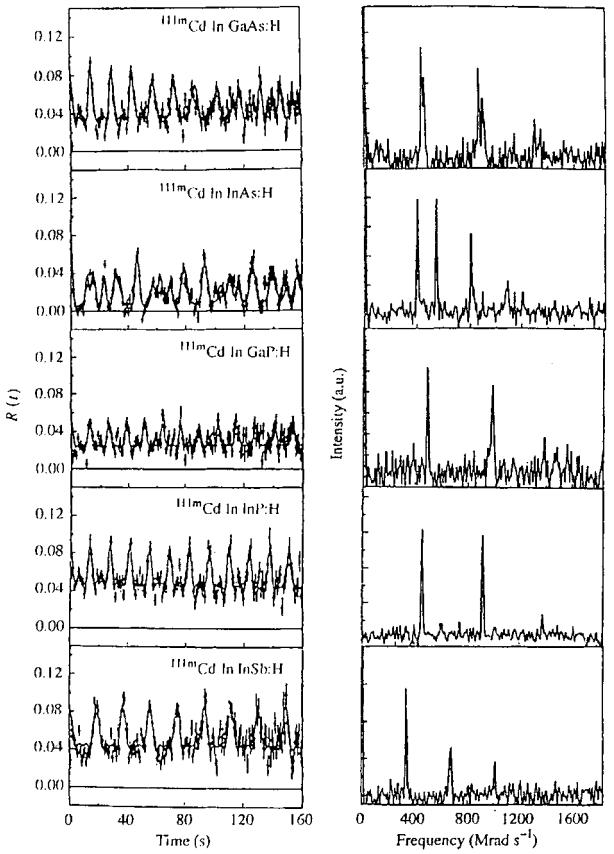

Figure 29. The results of perturbed angular correlation measurements on Cd-doped, plasma-charged III – V semiconductors. The probe atom ^{111m}Cd was used. On the left-hand side we see the raw differential time spectra [56] for the various semiconductors studied. On the right we see the corresponding Fourier transforms from which one can deduce the different electric field gradients at the sites of implantation of the radioactive ions.

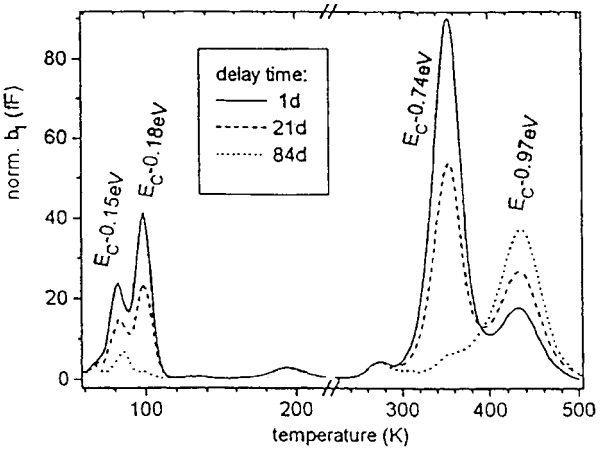

Figure 30. Deep level transient spectroscopy as a function of time for ^{51}Cr (half-life = 27.7 d) ions implanted into n-type 4H – SiC.

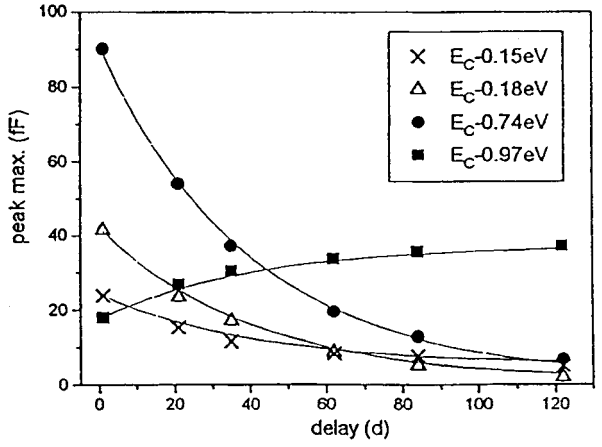

Figure 31. The decay of the peak heights of the spectroscopic features seen in figure 30. Three of them decay with the half-life of the implanted ^{51}Cr and one grows in with this half-life and is associated with the daughter (^{51}V).

properties but not their chemical identity. One such technique is DLTS. The 3d transition metals, especially V, Cr, Tic and Fe are frequent impurities in SiC crystals. The element V is also deliberately introduced to produce semi-insulating material. Clearly there is a strong interest in trying to identify the deep levels of these particular elements. This can be done by introducing a suitable radioactive species by implantation. In figure 30 we see the DLTS spectrum [58] from a sample of n-type 4H – SiC implanted with ^{51}Cr ions, which have a half-life of 27.7 days. We see the spectrum at three different times after implantation. Four distinct spectroscopic features are visible. Figure 31 shows the peak intensity for each of these features as a function of time. The solid lines represent exponential fits to the data points. Three of the curves reflect the ^{51}Cr half-life perfectly and the other fits the corresponding growth of the ^{51}V daughter. Accordingly the first three are due to a defect involving at least one Cr atom. The fourth involves vanadium. This radiotracer-DLTS method eliminates the guesswork in determining the chemical identities of the defects.

In a similar way we can modify an optical technique such as photoluminescence (PL) spectroscopy. Figure 32 shows the first PL spectra [59] for n-type Si implanted with 60 keV ions of ^{191}Hg and ^{195}Hg at CERN-ISOLDE. These isotopes decay into ^{191}Ir and ^{195}Pt respectively. After the decay the implantation damage was removed by annealing the samples for 5 s at 1173 K. The spectra revealed lines which had been assigned in the literature to Ag (for ^{191}Pt) [60] and Fe (for ^{195}Au) [61]. However it was found that the 'Ag' and 'Fe' half-lives decreased in intensity with the half-lives of ^{191}Pt and ^{195}Au respectively. It seems probable that the line commonly assigned to Fe is due to Au – Fe complexes, and

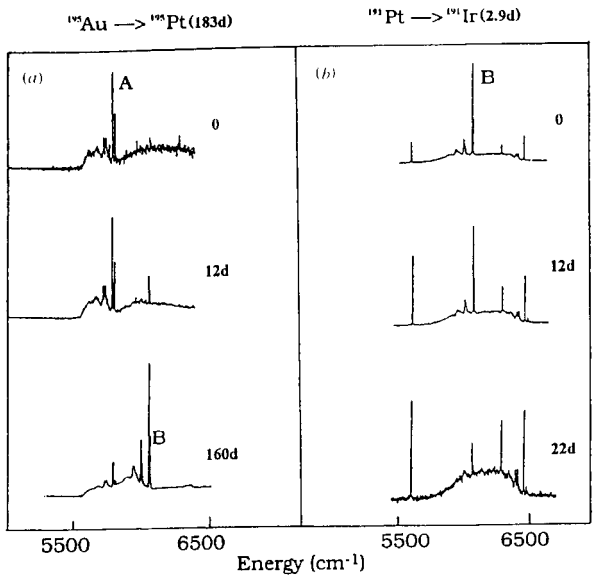

Figure 32. Photoluminescence spectra of Si doped with ^{191}Pt and ^{195}Au at three different times. The *x* axis shows the photon energy. In both cases the time dependence of the spectra is clear. Part (*a*) shows the chemical transformation of ^{195}Au to ^{195}Pt and (*b*) the transformation of ^{191}Pt to ^{191}Ir.

that the 'Ag' line is Pt related. However more experiments on radioactive Au and Pt in Si are required for an unambiguous interpretation. Nevertheless the great advantage of using radioactive ions to extract chemical information is clearly evident from these two examples. The method can be extended quite widely.

4.3.3. *Positron annihilation studies.* ISOL facilities (see section 2) also offer the possibility of creating high emissivity, high intensity sources of positrons for use in studies of materials and atomic physics. Facilities based on spallation or fission produce a very wide range of nuclear species. In parallel with the beam separated out by mass to be accelerated to the Coulomb barrier we can separate positron emitters and collect them by stopping them in a moderator. We can then produce essentially mono-energetic positron beams of energies controllable in the range of 1 eV to 400 keV by work function re-emission from the moderator surface. The efficiency of conversion from fast to slow positrons can be enhanced if nuclides with average energies lower than those used in laboratory systems, usually ^{22}Na, are employed. With beams of a positron emitter of 10^{11} per second one can deliver 10^{8} slow positrons per second to the entrance port of an experimental station. This would allow one to create continuous or pulsed positron beams which can be used for studies of subsurface regions, interfaces, thin films, surface spectroscopy, microscopy and atomic physics. A single example of how we might use these beams must suffice.

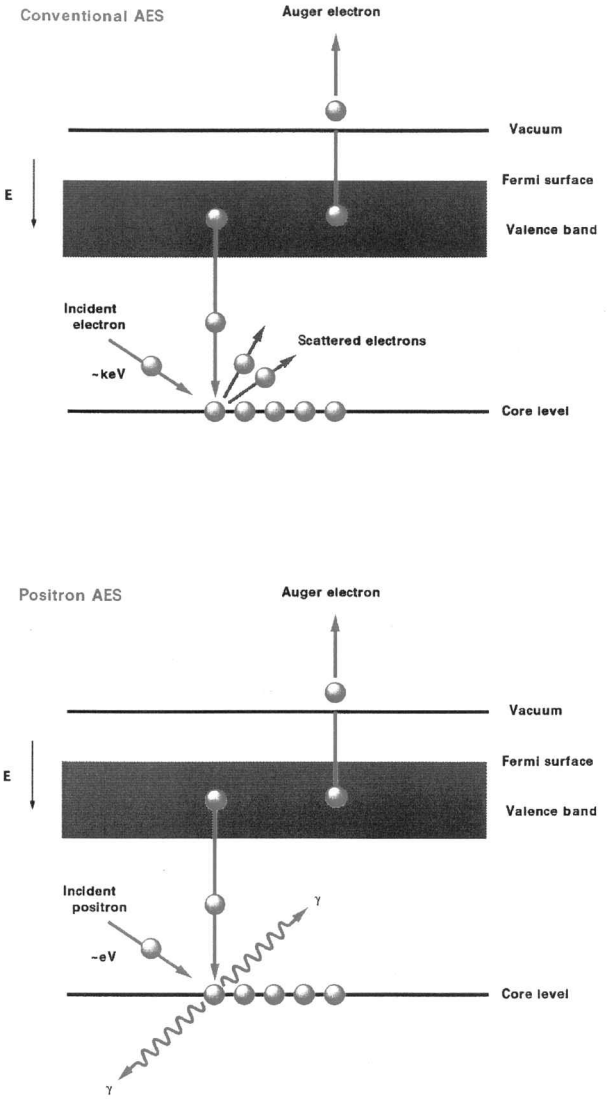

Figure 33. A comparison of conventional Auger electron spectroscopy (AES) with positron annihilation-induced Auger electron spectroscopy.

Auger electron spectroscopy (AES) is illustrated in figure 33. It is widely used to study defects in crystalline solids. If one uses positron-induced Auger electron spectroscopy (PAES) the low energy positrons create a hole in the core level of an atom by annihilation rather than by energetic impact. This is followed by Auger electron emission in the subsequent atomic rearrangement. PAES has the advantage over AES of (i) extreme surface sensitivity, (ii) reduction of dark noise by Auger electron-annihilation radiation gamma coincidences, (iii) negligible secondary electron background and (iv) the relatively low charge doses and low incident beam energy required for the study of fragile and insulating systems. The performance would equal that of AES but with these advantages. It would allow time-dependent studies of ultra-thin film

growth, higher resolution studies of Auger lineshapes, and studies of higher energy, and hence less probable, Auger peaks from heavier species. Surface segregation, H-termination and oxidation can all be studied with extreme surface sensitivity.

4.4. *Bio-medical, environmental and other applications*

Nuclear techniques have found widespread use in medicine for both diagnosis and therapy. In many of these applications one uses the radionuclides as tracers but in others one uses their decay properties for imaging or other purposes. The same techniques are ideal for the study of tribology and environmental problems.

Until now radioactive tracer applications *in vivo* have not been fully exploited because of the limited number of tracers available. Radionuclides which emit β^+ particles provide the basis for positron emission tomography (PET), and β^- emitters have great potential in the field of radionuclide therapy. PET [62] relies on the fact that when positrons annihilate the two 511 keV gamma rays produced are emitted back-to-back. Thus one can pinpoint a positron source in three dimensions with a detection system which is designed to detect the 511 keV gamma rays emitted at 180° to one another in prompt time coincidence. In medical applications of PET to date it is mainly used with short-lived species of C, N and O, which are ubiquitous in the body. They are created with beams from a small cyclotron. They are incorporated into biologically active molecules which are then introduced into the body where they are carried naturally to the brain or any other part of the body. We can then determine where this 'tagged' material ends up using PET. Figure 34 shows PET images taken [63] at PSI, Zurich by scientists from the Universities of Groningen and Surrey. Here ^{18}F nuclei have been incorporated into fluorodeoxyglucose to allow the study of metabolic rate in the brains of both control subjects and subjects with Alzheimer's disease. In figure 34 we see reconstructed images of the brain of a control subject ((*a*) and (*b*)) and two subjects with mild (*c*) and severe (*d*) Alzheimer's disease. The higher the metabolic rate the lighter the image in figure 34. In the case of the Alzheimer's sufferers clear metabolic deficiencies are seen in the frontal, parietal and temporal regions of the brain. From the pictures alone we can see how powerful a technique PET is. To date its use has been limited to a relatively small number of light elements. As a research tool PET has found widespread use in blood flow studies, glucose metabolism and neurological studies. It also shows great promise for use in clinical applications to the modern epidemics of cancer detection, cerebral dysfunction and heart disease. One would like to extend the use of PET to other essential trace elements in the body such as Se, which have a specific biological function. This requires ISOL facilities (see section 2) producing significant amounts of a wide range of carrier-free samples of radioactive ions of the relevant chemical elements.

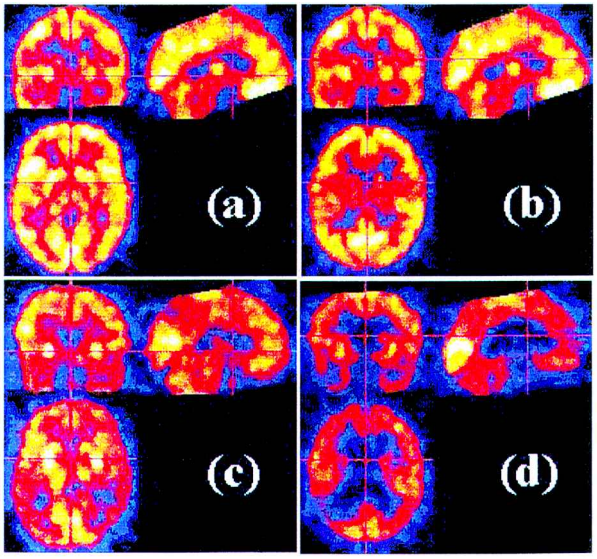

Figure 34. Positron emission tomography scans of the brains of a control subject ((*a*) and (*b*)) at two different *Z* coordinates and two subjects with symptoms of mild (*c*) and severe (*d*) Alzheimer's disease. The brighter the colour the higher the level of glucose metabolism. It is evident that there is a greater degree of glucose metabolism in the case of the control subject. (Courtesy of D. Cutts and N. Spyran.)

For the purpose of therapy it is essential to have carrier-free isotopes, and with the exception of ^{33}P, ^{89}Sr, ^{90}Y, ^{125}I and ^{130}I, the beta emitters of therapeutic interest are not commercially available. Since therapeutic effects depend critically on the specific activity, the systematic study of the relationship between the specific activity and biological response is an important topic for clinical research. New ISOL facilities based on fission or spallation will be able to produce a wide range of β^- emitters carrier-free and in quantities meeting clinical requirements. This will include a range of radio-lanthanides (^{153}Sm, ^{153}Gd, ^{151}Eu, ^{147}Eu, ^{143}Pr and ^{149}Pr), which are known to be non-specific 'tumour-seeking' tracers. The availability of isotopes with different half-lives would allow studies of the relationship between physical half-life and biological response. These β^--emitting isotopes chelated with various, low molecular weight ligands such as EDTMP, DTPA, etc. or labelled bio-conjugated compounds (bio-specific receptor seeking compounds with a defined sequence of amino acids) or monoclonal antibodies (bio-specific macromolecular protein compounds) can be used for such studies. These 'biological missiles' carry the radioactive isotopes selectively to the cancer cells. The radiation emitted in radioactive decay then destroys the cancer cells. The high purity and specific activity of the beams from ISOL facilities are essential to this application.

Among the greatly increased variety of carrier-free isotopes available from future ISOL facilities would be a range of intermediate mass, alpha-emitting nuclides such as ^{149}Tb. The use of this isotope offers the possibility of a superior approach to the control of early stage cancer or leukaemia. Alpha particles require two orders of magnitude fewer hits to kill a cell than beta particles. At the same time the alpha particles from ^{149}Tb have the shortest range known, which limits damage to surrounding tissues. Uptake of monoclonal antibodies, to which the ^{149}Tb must be attached, in solid tumours takes 24–48 h. The 4.1 h half-life of ^{149}Tb makes it unsuitable for attacking solid tumours. In contrast, uptake times for cells in transit or pre-angeogenic lesions are expected to be short and here the short half-life of ^{149}Tb may be a real advantage.

Our knowledge of the effects of trace elements in the body is very limited and is the subject of growing interest and research. One of the most sensitive analytical methods [64] for determining the presence of isotopic species is accelerator mass spectroscopy (AMS). It is widely used for ^{14}C dating with detection limits of 1 in 10^{15}. Aluminium is extremely difficult to detect in samples of body fluids or tissue because of contamination of samples. However the use of long-lived ^{26}Al (7×10^5 yr) as a tracer [65] has been very successful. The long half-life has meant a minimal activity administered to the patient. Suitable long-lived isotopes ($T_{1/2} > 10^5$ yr) exist for some twenty elements of interest including Mn, Fe, Ni, Se and various lanthanides. They should be produced carrier-free in sufficient quantity with new ISOL facilities to be ingested in suitable form and then the AMS technique can be used to determine their distribution in the body.

Studies of such elements in the body are important in terms of both toxicity and deficiency and a knowledge of their speciation is largely non-existent. Many of the techniques involving radioactive ions which have been developed for materials studies may find applications in bio-medicine. Perturbed angular correlations (PAC) can clearly be used for speciation studies. For example, ^{75}Se ($T_{1/2} = 120$ days) has been used to study the nature of the binding site of Se in a variety of biological samples. Again new ISOL facilities should provide carrier-free supplies of suitable isotopes to study many of the trace elements of interest.

The discovery of fullerenes opened many exciting possibilities. This is partly because of their exceptional stability and partly because the outer surface can be easily manipulated for different applications. It is possible to implant a radioactive atom of choice into a fullerene. They can be used as a vehicle to carry the radionuclide to the target in the human body for either diagnostic or therapeutic purposes. Already ^{99m}Tc@C_{60} has been suggested as an important species in the technecium gas generator used in lung tomography. One can visualize producing endohedral fullerenes with radioactive ions trapped inside by bombarding pre-formed fullerenes with a chosen beam of separated radioactive ions with high intensity but very low kinetic energy. This would open the way to a wide range of tests of fullerenes as 'magic bullets'. One can also visualize very similar uses for calixerenes loaded with radioactive ions. The fact that they are smaller than fullerenes may make them more suitable for some applications.

4.5. *Tribology*

Tribology will also benefit from the availability of a 'free choice' of radioactive ions for application. Wear on moving machine parts determines their lifetime, their fitness for purpose and the economics of their use. Precise measurements of wear resistance can be made by implanting radioactive nuclei into the material of interest. The wear of the part can then be monitored *in situ* by a measurement of the radioactivity, if the dose–depth distribution of ions is known. It is a method of great simplicity, which can be applied to ball bearings, turbine blades, piston rings, ceramics, etc. Given a wide range of radioactive ion beams the method has some advantages. It gives a choice of the appropriate chemical properties, half-life (short for research and development and long for field tests), the decay properties to be measured and the implantation depth. In addition to testing existing components this will allow one to compare the merits of different materials for a particular purpose.

Although man-made radioactive material constitutes on average less than 0.7% of human exposure to radiation in the UK, it is nevertheless important to minimize this exposure and one must take cognisance of the fact that it may be concentrated in some location or some part of the environment. Although there is considerable concern about the possible leakage of long-lived fission products from stored high level waste (HLW) from nuclear reactors it is not the only possible source of contamination. For example the main source of ^{99}Tc in the environment is as waste products from medical use of ^{99m}Tc.

Following the reprocessing of nuclear fuel the HLW can be isolated and stored by incorporating the material in various solid waste forms such as glasses, ceramics and phosphates, or by storing the fuel as UO_2 pellets clad in zircaloy. In either case it is planned to contain the material with barriers such as concrete containers including host phases like apatite. If one is to develop strategies to prevent contamination of storage facilities, soil, ground water, etc. then a detailed knowledge of the transport mechanisms of the relevant radionuclides is required. We need to know chemical speciation factors and devise isolation and containment methods for each of the isotopes concerned. Such information is required not just for the isotopes themselves but their daughter products as well.

The storage materials used for HLW can be investigated by implanting ions of radioactive fission products. Ion implantation allows one to introduce well known concentrations of specific fission products at given depths by varying the energy and intensity of the ions. One can then follow the evolution of these implants as a function of radiation dose, temperature, time and other factors. In the real storage conditions the radionuclides of importance are typically long-lived fission products. ISOL beams will allow one to implant shorter-lived isotopes of the same chemical element and hence undertake a speeded-up simulation of the processes of interest. In addition some of the radionuclides of interest in HLW, such as ^{90}Sr, ^{99}Tc and ^{106}Ru, emit no gamma rays or very few. Since gamma rays are easy to detect and highly specific in character, it is much easier to trace a short-lived isotope with suitable gamma emission and a daughter activity as well. Thus, for example, the ^{92}Sr (2.7 h) – ^{92}Y (3.5 h) chain, which would be produced abundantly by ISOL facilities based on proton spallation, is an excellent surrogate for ^{90}Sr.

The changes induced in storage materials can be characterized and followed by the Mössbauer effect or emission channelling, and by absorption techniques such as EXAFS and XANES. Microsectioning techniques can be used to determine radiotracer profile distributions.

Another strategy which has been proposed [66] to deal with radioactive waste is transmutation by neutrons created by the spallation of high energy protons. The simple idea is to transform the waste not to stable material but to a mix of radioactive species which is shorter-lived, less toxic and has a much smaller fraction of fissioning material. Naturally to proceed with such ideas we require a great deal of information on cross-sections and recoil momenta of residues for high-energy protons impinging on many radioactive species. This can be done by studying the inverse reactions, i.e. the results of allowing these radioactive species to impinge on a hydrogen target. Such studies have been carried out [68] at GSI. They are aimed at determining the radioactive pollution and material damage we can expect in a spallation source. At the same time these experiments shed light on the production of radioactive nuclei in spallation; information vital for understanding radioactive beam production.

5. Conclusion

The author hopes that the above gives his readers a flavour of the excitement created by the possibility of having beams of radioactive nuclei. The applications outlined above are, of course, only the tip of the iceberg. As stated earlier the examples given of how we would use radioactive beams are limited by our present knowledge and imagination. One can readily see further technical developments, which will create other new possibilities not discussed above. For example there have been a number of proposals to create electron storage rings alongside heavy ion storage rings so that one can study electron – nucleus interactions with intersecting beams. This would allow *inter alia* measurements of nuclear charge radii for nuclei far from stability. In a similar way one could arrange to have interactions between synchrotron radiation or thermal neutrons and exotic nuclei. All of these developments will lead to new applications.

Because of space constraints we have deliberately not discussed how radioactive ions can be used to test fundamental symmetries and the standard model of particle physics. For those interested a brief discussion of this topic can be found in [68].

Over the next five years or so a number of radioactive beam facilities based on the ISOL method will come on-line and the upgrade of current in-flight facilities will be completed. We can then expect to gather a rich harvest of results over a wide range of science.

References

[1] Ravn, H. L., 1998, *Phil. Trans. Roy. Soc.* (London), **A356,** 1955.
[2] Morrissey, D. J., and Sherrill, B. M., 1998, *Phil. Trans. Roy. Soc.* (London), **A356,** 1985.
[3] Sherrill, B. M., Morrisey, D. J., Nolen, J. A., and Wineer, J. A., 1991, *Nucl. Instrum. Meth. Phys. Res.*, **B56/57,** 1106.
[4] Mueller, A. C., and Anne, R., 1991, *Nucl. Instrum. Meth. Phys. Res.*, **B56/57,** 559.
[5] Geissel, H., *et al*., 1992, *Phys. Rev. Lett.*, **68,** 3412.
[6] Nolden, F., *et al*., 1997, GSI-Nachrichten 1/97,
[7] Stöhlker, T., *et al*., 1993, *Phys. Rev. Lett.,* **71,** 2184; Beyer, H. F., *et al*., 1995, *Z. Phys.*, **D35,** 169.
[8] Irnich, H., *et al*., 1993, *Phys. Rev. Lett.*, **75,** 4182; Schlitt, B., *et al*., 1996, *Hyp. Int.,* **99,** 117.
[9] Jung, M., *et al*., 1992, *Phys. Rev. Lett*., **69,** 2164.
[10] Stöhlker, T., 1998, *Hyp. Int.*, **115,** 129.
[11] Gorschkov, V. A., *et al*., 1993 *Proceedings of the 3rd International Conference on Radioactive Nuclear Beams*, edited by D. J. Morrissey (Gif-sur-Yvette: Editions Frontieres), p. 81.
[12] Tanihata, I., 1997, *Nucl. Phys.*, **A616,** 56c.
[13] See e.g. Ravn, H. L., 1986, *ISOLDE User's Guide*, edited by H. J. Kluge, CERN 86-05.
[14] Habs, D., *et al*., 1997, *Nucl. Instrum. Meth. Phys. Res.*, **B126,** 218.
[15] Nazarewicz, W., Sherrill, B., Tanihata, I., and Van Duppen, P., 1996, *Nucl. Phys. News*, **6,** 17.
[16] See 2000, Scientific Opportunities with Fast Fragmentation Beams from the Rare Isotope Accelerator, MSU Report, March (USA: MSU).
[17] See Dendooven, P., 1997, *Nucl. Inst. Methods,* **B126,** 182.
[18] Beausang, C., and Simpson, J., 1996, *J. Phys.*, **G22,** 527.
[19] Twin, P. J., *et al.*, 1986, *Phys. Rev. Lett.*, **57,** 811.
[20] Al-Khalili, J. S., and Tostevin, J. A., 1996, *Phys. Rev. Lett.*, **76,** 3903.
[21] See e.g. Nilsson, S. G., *et al*., 1969, *Nucl. Phys.*, **A131,** 1.
[22] Hofmann, S., *et al*., 1995, *Z. Phys.*, **A350,** 277; 1995, *ibid.*, **A350,** 281; 1996, *ibid.*, **A354,** 229.
[23] See Hofmann, S., 1998, *Rep. Progr. Phys.*, **61,** 639.
[24] ller, P. M., *et al*., 1995, *Nucl. Data Tables*, **59,** 185.
[25] Smolanczuk, R., 1999, *Phys. Rev.* C59, 2634
[26] Ninov, V., *et al*., 1999, *Phys. Rev. Lett.*, **83,** 1104.

[27] Oganessian, Yu., *et al*., 1999, *Phys. Rev. Lett.*, **83,** 3154; Oganessian, Yu., *et al*., 2000, *Phys. Rev.,* **C62,** 041604 (R); Oganessian, Yu., *et al*., 2000, *Phys. Rev.,* **63,** 011301 (R).
[28] Turler, A., *et al*., 1999, *Angew. Chem. Int. Ed.*, **38,** 2212.
[29] Janas, Z., *et al*., 1999, *Phys. Rev. Lett.*, **82,** 295.
[30] See Robertson, J. D., *et al*., 1990, *Phys. Rev.*, **C42,** 1922 and references therein
[31] Blank, B., *et al*., 1995, *Phys. Rev. Lett.*, **74,** 4611.
[32] Benenson, W., *et al*., 1975, *Phys. Lett.*, **B58,** 46.
[33] Kekelis, G. J., *et al*., 1978, *Phys. Rev.*, **C17,** 1429.
[34] Holt, R. J., *et al*., 1977, *Phys. Lett.*, **B69,** 55.
[35] Myers, W. D., 1989, *Proceedings of the 1st International Conference on Radioactive Beams*, Berkeley, CA, edited by W. D. Myers, J. M. Nitschke and E. B. Norman (Singapore: World Scientific), p. 269.
[36] Schneider, R., *et al*., 1994, *Z. Phys.*, **A348,** 241; Lewitowicz, M., *et al*., 1994, *Phys. Lett.*, **B322,** 20.
[37] Engelmann, Ch., and A. N. Other, 1995, *Z. Phys.*, **A352,** 351.
[38] Blank, B., *et al*., 2000, *Phys. Rev. Lett.*, **84,** 1116.
[39] Orr, N., Lecture Notes 'Ecole Internationale Juliot-Cure', Report (France: Université de Caen), LPCC 01-02.
[40] Smolanczuk, R., and Dobaczewski, J., 1993, *Phys. Rev.*, **C48,** R2166; Dobaczewski, J., Hamamoto, I., Nazarewicz, W., and Sheikh, J., 1994, *Phys. Rev. Lett.*, **72,** 981; Dobaczewski, J., *et al*., 1995, *Phys. scripta*, **T56,** 15.
[41] Dobaczewski, J., and Nazarewicz, W., 1998, *Phil. Trans. Roy. Soc.* (London), **356,** 2007.
[42] Lister, C. J., *et al*., 1987, *Phys. Rev. Lett.*, **59,** 1270.
[43] Burbidge, E. M., Burbidge, G.R., Fowler, W. A., and Hoyle, F., 1957, *Rev. mod. Phys.*, **29,** 547; Wagoner, R. V., 1973, *Astrophys. J.*, **179,** 343; Fowler, W. A., 1984, *Rev. mod. Phys.*, **56,** 159.
[44] Rolfs, C., and Rodney, W. S., 1988, *Cauldrons in the Cosmos* (Chicago: Chicago University Press).
[45] Rolfs, C., and Barnes, C. A., 1990, *Ann. Rev. Part. Nucl. Sci.*, **40,** 45.
[46] Wiescher, M., Schatz, H., and Champagne., A. E., 1998, *Phil. Trans. Roy. Soc.* (London), **A356,** 2105.
[47] Wiescher, M., 2000, *The Nucleus: New Physics for the New Millenium*, edited by Smit , F. D., Lindsay, R., and Foertsch, S. V. (New York: Kluwer Academic/Plenum Publishers), p. 467.
[48] Arnould, M., and Takahashi, K., 1999, *Rep. Progr. Phys.*, **62,** 393.
[49] Decrock, P., *et al*., 1991, *Phys. Rev. Lett.*, **67,** 808.
[50] Page, R. D., *et al*., 1994, *Phys. Rev. Lett.*, **73,** 3066.
[51] Wiescher, M., Gorres, J., and Thielemann, F. K., 1988, *Astrophys. J.*, **326,** 384.
[52] Garcia, A., *et al*., 1991, *Phys. Rev.*, **C43,** 2012; Sherr, R., and Fortune, H. T., 1998, *Phys. Rev.*, **C58,** 3292.
[53] Alton, G. D., and Beene, J. R., 1998, *J. Phys.*, **G24,** 1347.
[54] Martinella, R., *et al*., 1985, *Mat. Sci. Eng.*, **69,** 247.
[55] Bardayan, D. W., *et al*., 1999, *Phys. Rev. Lett.*, **83,** 45.
[56] Baurichter, A., *et al*., 1991, *Appl. Surf. Sci.*, **50,** 165; Baurichter, A., *et al*., 1992, *Mat. Sci. Forum*, **83–87,** 593.
[57] Forkel-Worth, D., 1998, *Phil. Trans. Roy. Soc.* (London), **A356,** 2137.
[58] Achtziger, N., *et al*., 1995, *Appl. Phys. Lett.*, **66,** 2370.
[59] Henry, M. O., *et al*., 1996, *Proceedings of the 23rd International Conference on Physics of Semiconductors*, Berlin, Germany, July, edited by M. Scheffler and R. Zimmerman (Singapore: World Scientific).
[60] Nazare, M. H., *et al*., 1989, *Mat. Sci. Eng.*, **B4,** 273.
[61] Docarmo, M. C., *et al*., 1989, *Defects in Semiconductors*, edited by G. Ferenczo (Aedermannsdorf: Trans. Tech. Publications), p. 1497.
[62] Myers, R., Cunningham, V., Bailey, D., and Jones, T. (eds), 1996, *Quantification of Brain Function using PET* (New York: Academic Press).
[63] Cutts, D. A., Maguire, R. P., Stedman, J. D., Leenders, K. L., and Spyrou, N. M., 1999, *Biol. Trace Elements Res.*, **71,** 541.
[64] See e.g. Kutschera, W., 1999, *Proceedings of Experimental Nuclear Physics in Europe*, Sevilla, *AIP Conference Proceedings 495*, edited by B. Rubio, M. Lozano and W. Gelletly (New York: AIP), p. 407.
[65] Day, J. P., *et al*., 1991, *Lancet*, **337,** 1345.
[66] Bowman, C. D., *et al*., 1992, *Nucl. Instrum. Methods Phys. Res.*, **A320,** 336.
[67] See e.g. Benlliure, J., *et al*. 1998, *Nucl. Phys.*, **A628,** 458.
[68] 1998, *SIRIUS Science*, report funded by EPSRC (ISBN 0-90376-75-6: CCLRC).